Developing a G-Protein Coupled Receptor Coupled Signaling System in Yeast with Improved Sensitivity for the Selection of Functional Modulators of Heterologous G-Protein Coupled Receptors

Sajinth Thampipillai

A Thesis
In the Department of
Biology

Presented in Partial Fulfillment of the Requirements
For the Degree of
Master of Science (Biology)

At Concordia University
Montreal, Quebec, Canada

August 2022

CONCORDIA UNIVERSITY

SCHOOL OF GRADUATE STUDIES

This is to clarify that the thesis prepared

By: Sajinth Thampipillai

Entitled: Developing G-Protein Coupled Receptor Coupled Signaling System in Yeast with Improved Sensitivity for the Selection of Functional Modulators of Heterologous G-Protein Coupled Receptors

and submitted in partial fulfillment of the requirements for the degree of

Master of Science (Biology)

complies with the regulations of the University and meets the accepted standards with respect to originality and quality.

Signed by the final examining committee:

_____Chair
Dr. Vincent Martin

_____External Examiner
Dr. Paul Joyce

_____Examiner
Dr. Aashiq H. Kachroo

_____Examiner
Dr. Vincent Martin

_____Thesis Supervisors
Dr. Cunle Wu and Dr. Malcolm Whiteway

Approved by

_____
Dr. Robert Weladji, Graduate Program Director

September 08, 2022

_____
Dr. Pascale Sicotte, Dean of Faculty

ABSTRACT

Developing a G-Protein Coupled Receptor Coupled Signaling System in Yeast with Improved Sensitivity for the Selection of Functional Modulators of Heterologous G-Protein Coupled Receptors

Sajinth Thampipillai

G-protein coupled receptors (GPCRs) are transmembrane proteins that are found at the plasma membrane in eukaryotes, where they direct responses to many environmental stimuli and control many aspects of cellular function. The similarity between pheromone signaling in yeast and GPCR-mediated signaling in humans has allowed the development of genetic and chemical high-throughput screening to isolate agonists or antagonists of GPCRs using yeast biosensors with functionally coupled heterologous GPCRs. This project aims to improve the signaling sensitivity of heterologous GPCRs in engineered yeast by introducing positive feedback loops (PBLs) consisting of primary signal-induced expression of critical regulators of the signaling pathway, such as adaptor protein Ste50 and scaffold protein Ste5. Ste50 and Ste5 were upregulated through overexpression of an inducible promoter that is controlled by the mating signal. A comparative analysis through a long-term assay and a short-term assay was used to test if the weak signaling of a GPCR can be amplified when compared to the wildtype. Our results show that for long-term assays the addition of Ste50 through the positive feedback loop supported increased reporter signaling whereas Ste5 alone and in combination with Ste50 caused Far1-independent cell cycle arrest. In short-term assays, the combined positive feedback loop system, Ste50 and Ste5 demonstrated higher levels of signaling, as compared to either one alone or the wildtype. This study presents a possible solution to increasing the reporter output of the yeast pheromone pathway with greater sensitivity through controlled positive feedback loops of two positive regulators.

ACKNOWLEDGEMENTS

I would like to thank the Department of Biology, Faculty of Arts and Science, Concordia University, Montreal for allowing me to pursue my graduate studies.

I would like to thank Dr. Cunle Wu for allowing me to work alongside him at the Research Center for Human Health Therapeutics, National Research Council Canada. I am extremely grateful for the encouragement and guidance he has provided me throughout the project.

I would like to thank Dr. Malcolm Whiteway for co-supervising me during my project and for his guidance and support throughout my studies.

I would like to thank Dr. Aashiq Kachroo and Dr. Vincent Martin for being part of my committee team and for providing the proper guidance on this project.

I would like to thank Audrey Morasse for training me on the flow cytometer during my time at the NRC.

I would like to thank Dr. Alisa Piekny and Mrs. Orly Weinberg for presenting this opportunity to me.

Lastly, I would like to thank my family and friends for their support during my time at the NRC and graduate studies.

TABLE OF CONTENTS

LIST OF FIGURES

LIST OF ABBREVIATIONS

AmpR	Ampicillin Resistance
dH_2O	Distilled Water
DNA	Deoxyribonucleic Acid
dNTPs	Deoxynucleotide Triphosphates
E.coli	*Escherichia coli*
GDP	Guanosine-5'-Diphosphate
GFP	Green Fluorescent Protein
GPCR	G-Protein Coupled Receptors
G-proteins	Guanine Nucleotide Binding Proteins
GTP	Guanosine-5'-Triphosphate
HDR	Homology-Directed Repair
HIS3	Imidazoleglycerol-Phosphate Dehydratase
LB	Lysogeny Broth
LEU2	Beta-Isopropylmalate Dehydrogenase
MAPK	Mitogen-Activated Protein Kinase
NHEJ	Non-Homologous End Joining
PAM	Protospacer Adjacent Motif
PBS	Phosphate-Buffered Saline
PBL	Positive Feedback Loop
PCR	Polymerase Chain Reaction
PH	Plextrin Homology
PM	Plasma Membrane
PRE	Pheromone Response Element

RA	Ras-Associating
RGS	Regulators of G-protein Signaling
SAM	Sterile Alpha Motif
S. cerevisiae	*Saccharomyces cerevisiae*
SD	Synthetic Dextrose
URA3	Orotidine-5'-Phosphate Decarboxylase
YPD	Yeast Extract-Peptone-Dextrose
3-AT	3-Amino-1,2,4-Triazole

CHAPTER 1: INTRODUCTION

1.1 G-Protein Coupled Receptors (GPCRs) and Their Therapeutic Potential

G-protein coupled receptors (GPCRs) are members of a superfamily of integral membrane proteins that respond to many stimuli and control many aspects of cellular functions and thus act as important therapeutic targets for many diseases[1]. All GPCRs have similar structure and the same topology consisting of a single polypeptide that spans the plasma membrane (PM) seven times with an extracellular N-terminus and an intracellular C-terminus[1,2] (**Fig 1**). Signaling is mostly done in response to an extracellular ligand that binds to an extracellular domain of the GPCR this binding will transmit the response internally, mediated through guanine nucleotide binding proteins (G-proteins)[3] (**Fig 1**). Despite their similarity in structure, GPCRs can specifically recognize a multitude of different stimuli such as pheromones, hormones, light, etc[1,4–7]. There are approximately 800 GPCRs in the human genome, and approved drugs target only 16% of them[8–10]. To date, approximately 35% of all clinically prescribed drugs function as agonists or antagonists targeting GPCRs[8,11,12]. Of the 35% of clinically prescribed drugs, 26% of the top sellers generated around 23.5 billion dollars in profits, which comprises 9% of the entire global market share for drugs[9,10,12,13]. Due to lengthy and expensive research and development processes, bringing new GPCR agonist or antagonist drugs to market has been challenging[10]. Any approaches improving the process of identification, characterization, or validation of the association between specific molecular targets and specific disease states will help reduce the complications in drug discovery and development[10]. As GPCRs are highly conserved in eukaryotes, the baker's yeast *Saccharomyces cerevisiae* has been one of the key model organisms used both to better understand and to modify the internal components of the pathway involved in GPCR signaling, and to provide

biosensor platforms to identify receptor ligands[14–20]. Thus, yeast can help bring novel drugs into the market as GPCR modulators.

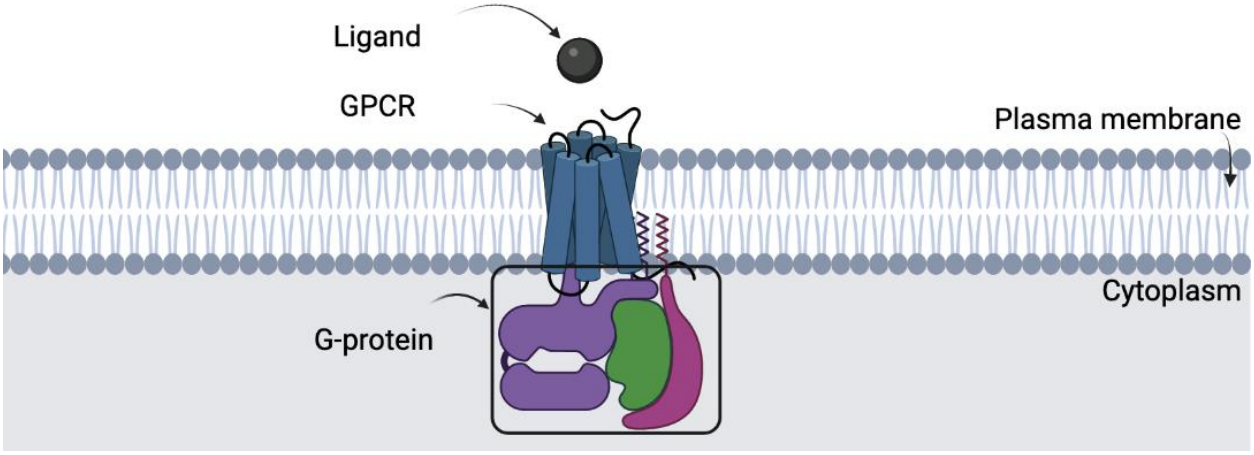

Figure 1. General structure of G-protein coupled receptors (GPCRs). The figure demonstrates the binding of a ligand (black sphere) to the extracellular component of the GPCR (blue rods) that span the plasma membrane of the cell. This membrane-spanning region is linked to the G-protein (α as purple, β as green and γ as red) to activate different downstream pathways. Adapted from refs[21–23]

1.2 GPCRs in the Budding Yeast *Saccharomyces cerevisiae*

The model organism *S. cerevisiae* is important for both biotechnology and biomedical research and has proven useful for studying human GPCRs signaling[24]. Some of the positive characteristics that have allowed yeast to be easily re-engineered include ease of handling, rapid and robust growth, genetic encodability, haploid stability and low cost[24]. *S. cerevisiae* contains two native GPCR-mediated pathways with one of them having two receptor sub-types[14]. The first is responsible for glucose sensing mediated by the Gpr1 receptor; the other (with the two sub-types) is the pheromone response pathway, also known as the mating pathway, and is responsible for pheromone sensing mediated by Ste2 or Ste3[25–28] (**Fig 2**).

The Gpr1 receptor controlling the glucose sensing pathway is expressed in both diploid and haploid cells and regulates the activity of Gpa2, a Gα subunit, in response to glucose, to direct filamentous growth (**Fig 2**)[26,28]. Candidate Gβ and Gγ subunits of a heterotrimeric G-protein from the glucose sensing pathway are non-classical and the signaling mechanisms are not well understood[29–31]. All three heterotrimeric subunits vary in structure compared to the heterotrimeric G-proteins found in mammalian cells or the yeast pheromone pathway. This includes a Gα subunit that contains an extended N-terminus and a G$\beta\gamma$ subunit containing seven kelch repeats with no sequence homology with the seven WD40 repeats found in G$\beta\gamma$ in other pathways[30,32–35]. These differences from the standard pathway have resulted in the glucose sensing pathway being less explored as a heterologous GPCR biosensor.

In the yeast pheromone pathway, the heterotrimeric G-protein is made up of subunits Gpa1, Ste4 and Ste18, and is similar in structure and functionality to the heterotrimeric G-protein found in mammalian cells consisting of Gα, β and γ subunits[21,36,37]. In addition, the activation of the heterotrimeric G-protein, in which guanosine-5' -diphosphate (GDP) is exchanged for guanosine-5' -triphosphate (GTP) on the Gα subunit, is similar between yeast and mammals[16,21](**Fig 2**). These similarities have allowed various mammalian GPCRs to be functionally coupled to the heterotrimeric G protein found in the yeast pheromone response pathway[16,21]. The primary focus of this project is to modify the yeast pheromone pathway to improve the signaling output and pathway sensitivity. This pathway uses a mitogen-activated protein kinase (MAPK) module to mediate the intracellular signal transduction downstream of GPCR/G-protein activation upon pheromone stimulation[16,21](**Fig 2**).

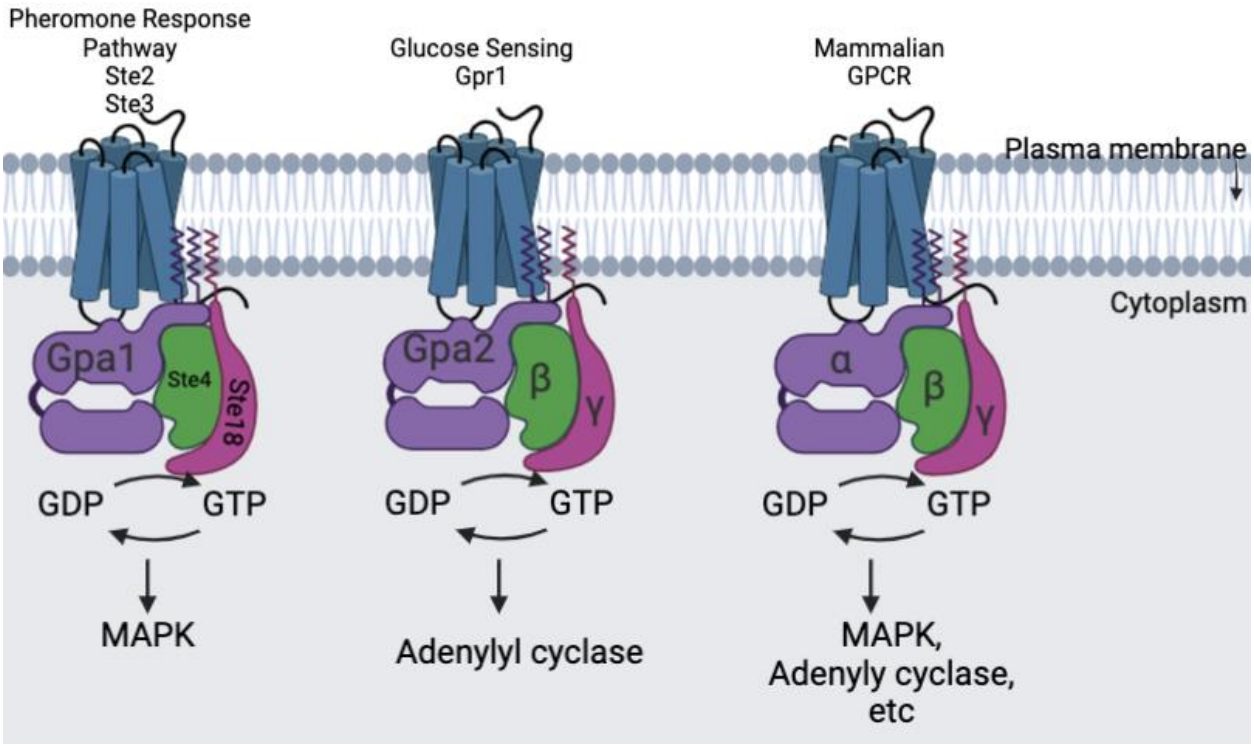

Figure 2. Yeast vs mammalian GPCRs. The figure demonstrates the similarities between GPCR/G-protein activation in yeast and mammalian cells. Once activated, the heterotrimeric G-proteins use different intracellular effectors to connect to many different downstream signaling pathways. Adapted from refs[21–23]

1.3 The Yeast Pheromone Response Pathway and the Different Components Involved in GPCR-Mediated Signaling

The yeast pheromone response pathway is one of the most well studied signal transduction pathways[15]. As previously mentioned, there are two subtypes of GPCRs in the mating pathway, the mating type **a** cell with the Ste2 receptor that gets activated by α-factor secreted by the opposite mating type α cell, and the mating type α cell with the Ste3 receptor that gets activated by **a**-factor secreted by **a** cells[27] (**Fig 3**). In the inactive state, GDP is bound to the Gpa1 subunit and forms a complex with the Gβ (Ste4) and Gγ (Ste18) subunits[36,37]. Upon activation, the exchange for GTP for GDP causes conformational changes in Gpa1 leading to the dissociation from the Ste4/Ste18 complex (**Fig 3**). The scaffold protein Ste5 creates a complex composed of inactive Ste11 kinase

bound to Ste50, plus kinases Ste7 and Fus3, and is recruited to the PM via its PM localization domain and interaction with Gβγ[38–41]. At the PM, Ste4/Ste18 (Gβγ) complex plays a critical role in the activation of the Ste20 kinase for transmitting a signal to the Ste5-scaffolded MAP kinase cascade[37–39,41–44] (**Fig 3**). A model for signal transduction in the MAP kinase cascade suggests that Ste20 first phosphorylates the MAPKKK, Ste11, potentially with the help of Ste50, which then phosphorylates the MAPKK, Ste7[39,40,42] (**Fig 3**). Ste7-mediated phosphorylation activates 2 different MAPKs, Fus3 that is bound to Ste5, and Kss1 that is bound to the transcription factor complex Ste12/Dig1/Dig2[39,41,45–47]. Fus3-mediated phosphorylation has multiple substrates, including the transcriptional factor complex Ste12/Dig1/Dig2, the Far1 protein that mediates cell cycle arrest, and the Bni1 protein that participates in cell polarization[41,45–49]. Phosphorylation of the transcription factor complex occurs by Fus3 and Kss1 resulting in the Dig1 and Dig2 regulators binding less tightly to the transcription factor Ste12, allowing it to enter the nucleus, and leading to the expression of many pheromone response genes through binding to the pheromone response element (PRE) motif[41,45–47,49]. Furthermore, phosphorylation and stabilization of Far1 leads to cell cycle arrest in the G1 phase; and interaction with free Gpa1 to phosphorylate polarisome components including Bni1 at the shmoo initiation site leads to cell polarization and shmoo formation[41,44,48,50,51] (**Fig 3**). Down regulation of the pheromone response occurs through either Sst2, a regulator of G-protein signaling (RGS), or Bar1, a secreted protease that degrades α-factor[52–55]. Previous studies suggest that Dig1 and Dig2 can also down regulate the pheromone pathway activity as a repressor of Ste12 transcriptional activity upon pheromone stimulation[45,46]. However, the phosphorylation events in the regulation of Ste12 need to be further explored and are not well understood. Modifications to the yeast pheromone pathway, such as gene knockouts

of the well-studied negative regulators, are beneficial in improving the signaling properties of the pathway which can help ligand detection.

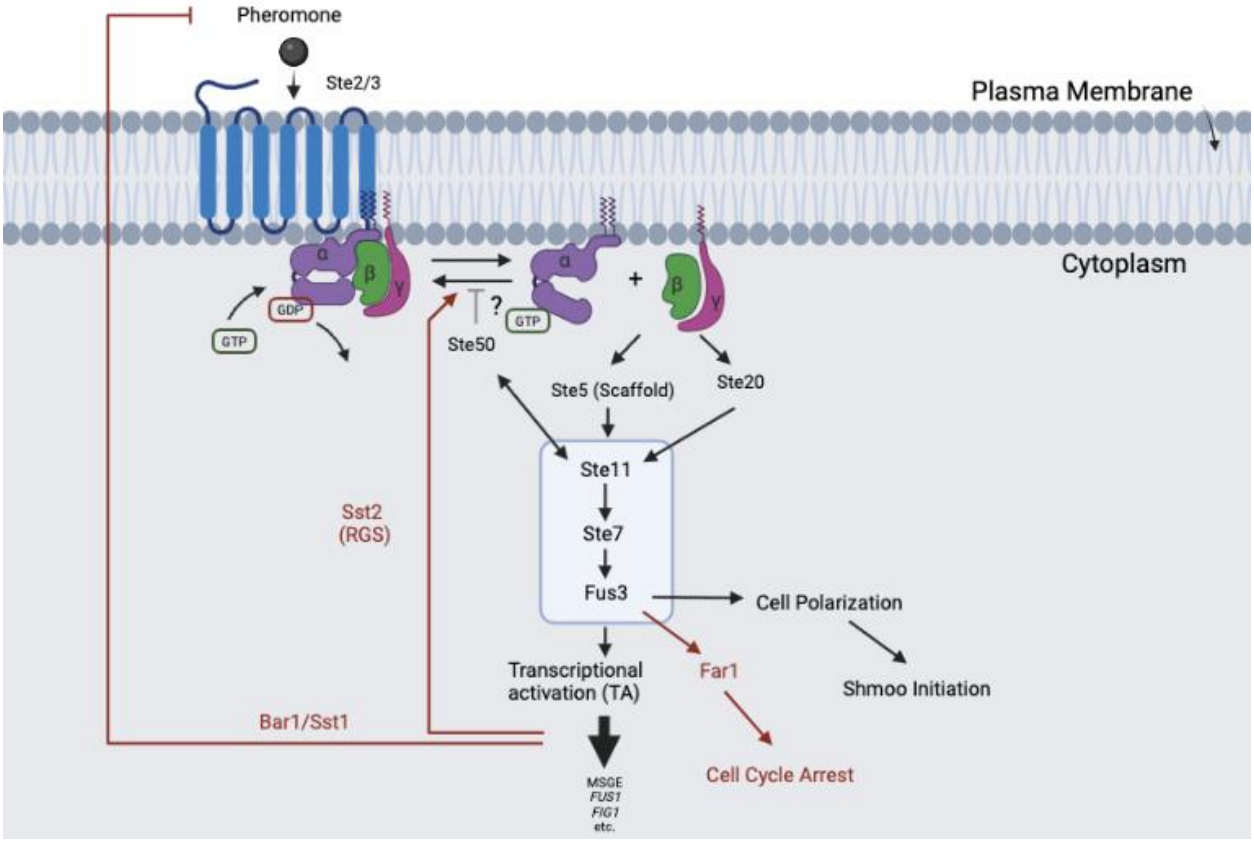

Figure 3. The important components of the yeast pheromone pathway. The figure demonstrates the general overview of the yeast pheromone pathway. Binding of pheromone activates the GPCR (Ste2/Ste3), which stimulates the exchange of GTP for GDP on the G*α* (Gpa1) protein leading to the dissociation of the Gβ/G*γ* complex. The dissociation in turn leads to the activation of the MAP kinase cascade composed of Ste11, Ste7 and Fus3. Activated Fus3 then phosphorylates transcriptional factor Ste12 leading to transcriptional activation, phosphorylates Far1 leading to cell cycle arrest and phosphorylates Bni1 for cell polarization at the shmoo initiation site. Adapted from refs[22,23,51,56].

1.4 Genetic Modifications to the Yeast Pheromone Response Pathway that Allow the Platform to be Used as a Biosensor

Previous studies have demonstrated several modifications to the pheromone pathway that allow GPCRs to be used as a means of detecting different ligands. The two most common disruptions to the pathway are the removal of the *SST2* and *FAR1* genes[21,48,52,53,55] (**Fig 4**). Sst2 is

the RGS equivalent in the yeast pheromone pathway and acts as the regulator of Gpa1[53,55]. By promoting GTP hydrolysis by stimulating the GTPase activity of Gpa1 leading to the inactive state of the G-protein, Sst2 acts as the principal negative regulator of the pathway and its deletion renders yeast cells hypersensitivity to pheromone[21,52,53,55,57]. As previously mentioned, *FAR1* is the gene that encodes the protein capable of leading to cell cycle arrest through Fus3-mediated phosphorylation followed by the inhibition of a G1 cyclin, Cln2[41,48,58,59]. Yeast cells lacking *FAR1* are unable to mediate cell cycle arrest in the presence of pheromone. Another negative regulator of the pathway is Sst1, also known as Bar1, an endoprotease whose expression is transcriptionally controlled by Ste12[47,54–56,60]. Specific to the mating type **a** cell, Bar1 protease secreted from the cell is capable of cleaving and thus inactivating α-factor to turn off the pheromone response pathway[54–56,60].

The addition of reporter genes to the pathway is critical for GPCR assays when measuring the signaling output. Some of the reporter genes used include *HIS3* for auxotrophic assay[61,62], green fluorescent protein (GFP*)* as a fluorescent reporter[63], and *LacZ* for colorimetric assay[64]; these are normally coupled with pheromone inducible promoters from such genes as *FUS1, FIG2*, and *FIG1*[65–67] (**Fig 4**). Lastly, for GPCR coupling to mammalian GPCRs, two modifications are required. The first is the replacement of the native Ste2 or Ste3 receptor with a heterologous GPCR[16] (**Fig 4**). The second is the replacement of the last 5 amino acid residues of Gpa1 with the last 5 residues of a human Gα, creating a chimeric Gα[16]. For many years, the described gene edits on the yeast pheromone pathway have been exploited and have become the standard in many heterologously expressed GPCRs[16,22]. However, further modifications to the pheromone pathway are needed, and these are currently being investigated through other means such as other gene knockouts or inserts, and overexpression of essential genes[22,65].

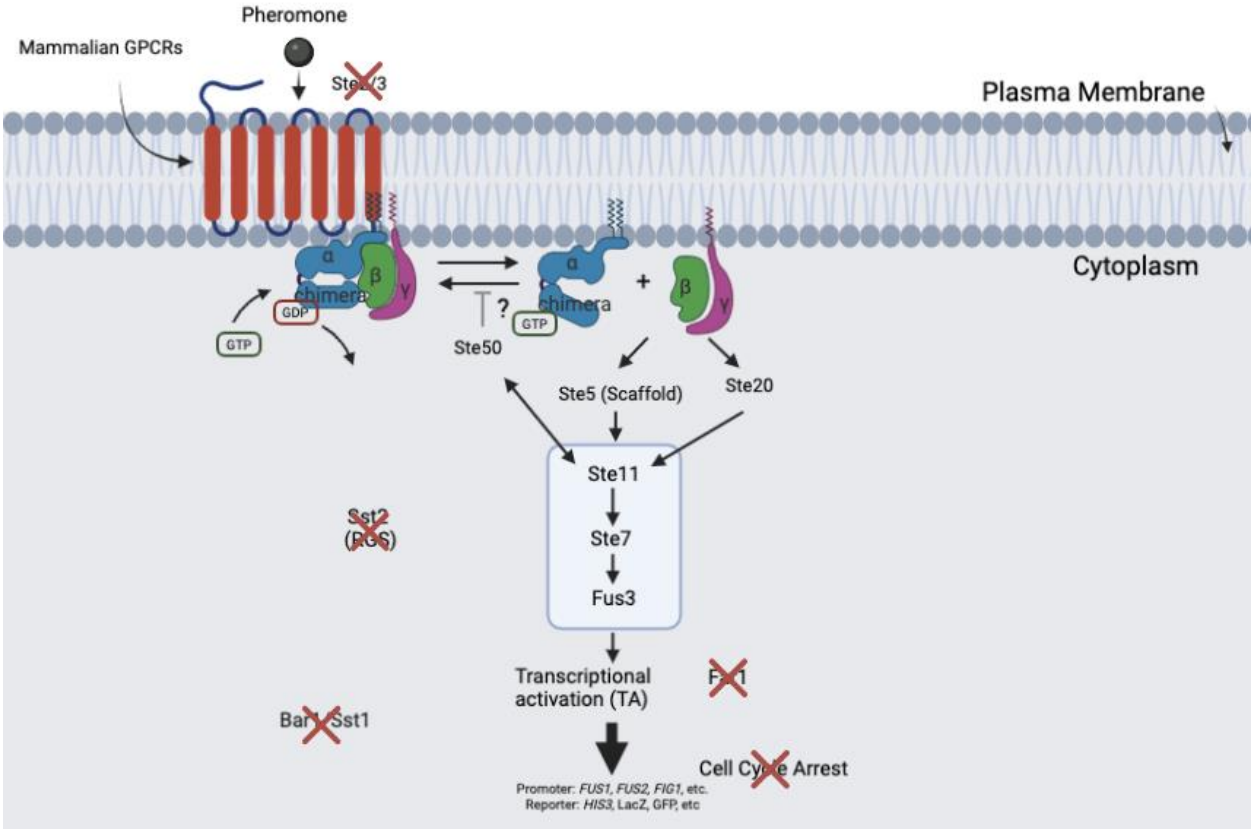

Figure 4. Engineered yeast pheromone pathway. Removal of the two negative regulators Sst2 and Sst1/Bar1, and the *FAR1* gene prevent cell cycle arrest from occurring, allowing for better detection of ligands, and improving pathway sensitivity. Replacing the native Ste2/3 GPCR receptor with a mammalian GPCR and swapping the last 5 amino acid residues of Gpa1 with the equivalent residues from a mammalian Gα ensures specificity of heterologous GPCR coupling. Adapted from refs[16,22,23,65]

1.5 Hypothesis and Objective of This Study

We hypothesize that introduction of positive feedback loops of positive regulators could improve the sensitivity of GPCR signaling in the pheromone response pathway. Two positive regulatory components of the yeast pheromone pathway to be explored are the adaptor protein Ste50 and the scaffold protein Ste5 as they have been demonstrated to be important components in signal transduction, with previous studies demonstrating that overexpression of these proteins had led to enhanced signaling[40,43,68–72] (**See green lines in Fig 5**). The *STE50* and *STE5* genes are engineered under the control of a pheromone-inducible promoter as it will allow for a better control

of their expression as opposed to consecutive overexpression that can potentially lead to high basal levels in the absence of ligand[71]. This activation system will allow Ste50 and Ste5 to be upregulated through transcriptional activation depending on ligand binding and pathway signaling.

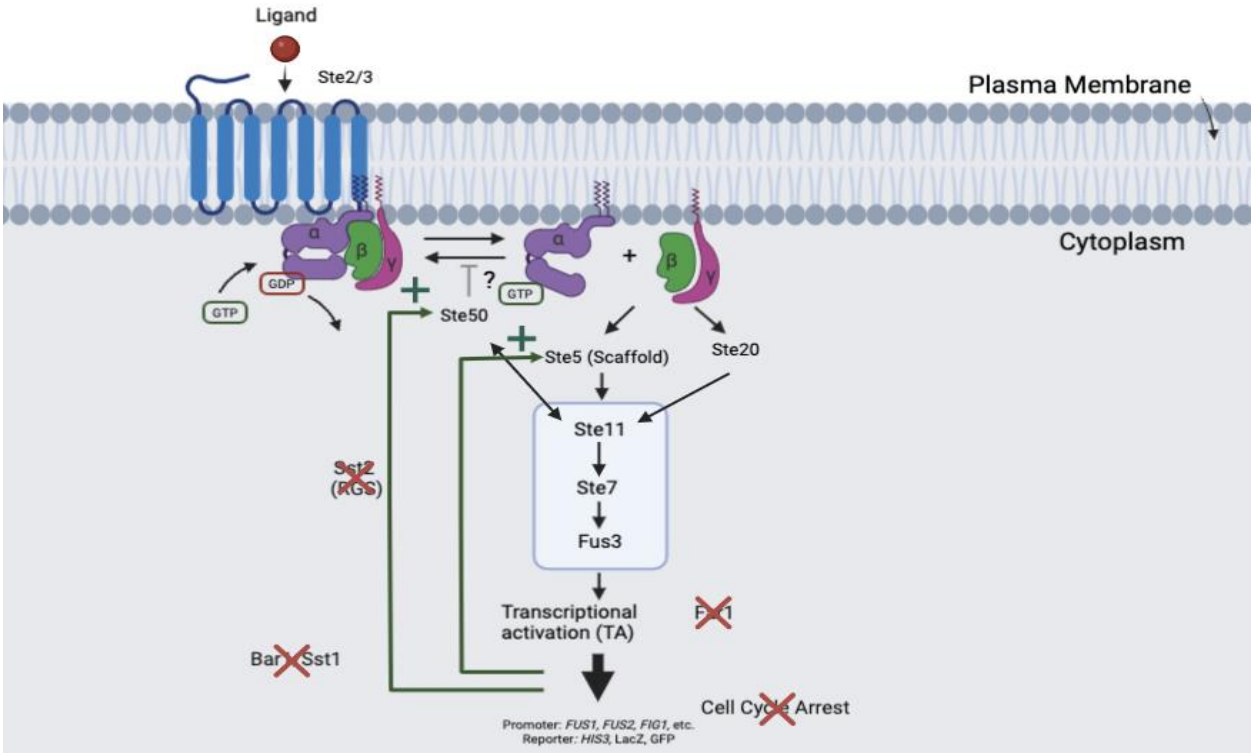

Figure 5. Introduction of positive feedback loops of Ste50 and/or Ste5. The figure depicts the addition of positive feedback loops into the yeast pheromone pathway to improve sensitivity of the ligand-induced signaling response. The adaptor protein Ste50 and the scaffold protein Ste5 are upregulated through promoters that are activated by the transcription factor Ste12 through the signaling of the pathway. Adapted from refs[22,23,65].

The adaptor protein Ste50 has regulatory functions involved in many signaling pathways found in yeast, including the mating pathway[40,68,69]. It is composed of 346 amino acids and contains two important domains: the N-terminal sterile alpha motif (SAM) domain and the C-terminal Ras association (RA)-like domain[40,69]. For Ste50 to function it requires both the N-terminal SAM domain to interact with Ste11 to aid its activation by Ste20 through phosphorylation, and the C-terminal RA-like domain which is shown to interact with component Opy2 for PM localization[40,69,73]. However, *ste50Δ* strains are partially defective in the four aspects of the mating

pheromone response pathway - pheromone-induced transcriptional activation, cell cycle arrest, diploid formation and shmoo formation[40,68].

The scaffold protein Ste5 is expressed in haploid cells and is critically important for the pheromone response pathways as it serves to prevent improper crosstalk amongst the different pathways found in yeast that use Ste11 and Ste7[39,74]. Ste5 is composed of 917 amino acids with an acidic C-terminus and a cysteine rich N-terminus, and it contains two small regions that have sequence similarity to Far1[43,75–77] (**Fig 6**). In the yeast pheromone pathway, Ste5 is responsible for assembling the protein kinases that are essential for mating signal transduction, so *ste5Δ* haploid cells are unable to respond to pheromone and unable to mate to form diploids, the so-called sterile phenotype[43,70,78]. As there is no evidence that Ste5, Ste11, Ste7 and Fus3 are transcriptionally regulated by pheromone signaling their function in the pheromone pathway is only activated when the kinase cascade is formed and proper spatiotemporal localization of the kinase cascade to G$\beta\gamma$ near the PM occurs[70,74,78]. Proper spatiotemporal localization requires the Ste5 N-terminal region to interact with G-$\beta\gamma$ unit upon activation[78]. Past studies have demonstrated that Ste5 positively regulates the pheromone pathway and that overexpression of *STE5* leads to increased Fus3 kinase activation[70,71]. In addition, Ste5 is rate limiting for activation of Fus3 as it won't get activated by Ste7 unless bound to Ste5 along with Ste11 and Ste7, making it an essential component of the MAPK cascade of the pheromone response pathway for signal transduction[70,78,79]. Another study demonstrated that the scaffold Ste5 can result in cell cycle arrest if degradation through ubiquitin and the proteasome is inefficient within the nucleus[71]. As Ste5 shares sequence similarity with Far1 in two small regions, the RING domain and one in the PH domain, it might mimic Far1's role in cell cycle arrest when over produced, suggesting that the level of Ste5 and its cellular localization are critically important in controlling pathway signaling.

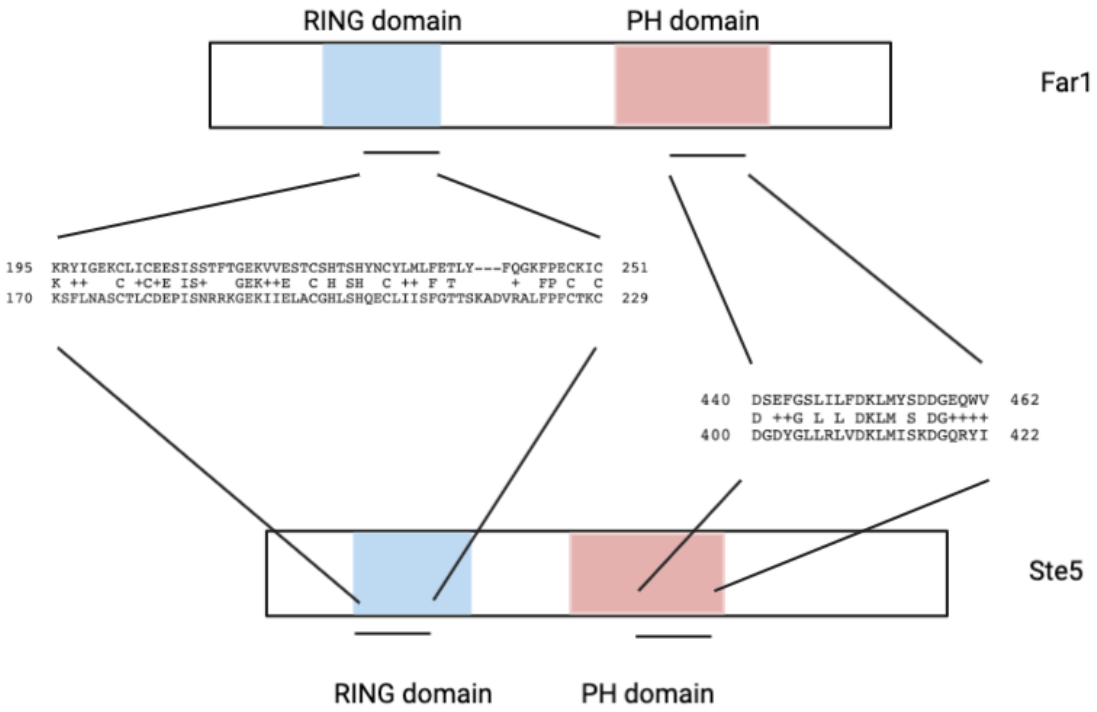

Figure 6. Alignment of regions of similarity between of Ste5 and Far1 scaffold proteins. Figure represents similar regions within the Ste5 and Far1 RING and PH domains. Adapted from refs[23,75–77].

In this study, we will build constructs in which *STE50* and *STE5* will be put under the control of inducible promoters such that their expression is transcriptionally induced by the signaling of the pheromone pathway. These positive feedback loops and their combination are expected to amplify weak GPCR signaling. The improved pheromone response pathway with increased sensitivity to ligand should help advance the drug discovery process by allowing researchers to pick up more potential leads for further testing and engineering, and to be developed as modulators of GPCR signaling.

CHAPTER 2: MATERIALS AND METHODS

2.1 Plasmid Construction

2.1.1 Cloning *STE50* Under the Control of Inducible Promoters

All plasmid constructs were generated and propagated in *Escherichia coli,* DH5-α (F⁻ *φ80lacZΔM15 Δ(lacZYA-argF)U169 recA1 endA1 hsdR17*(r_K^-, m_K^+) *phoA supE44 λ⁻thi-1 gyrA96 relA1*) or MC1061 (F⁻ *Δ(araA-leu)7697, [araD139]*$_{B/r}$, *Δ(codB-lacI)3, galK16, galE15(GalS), λ⁻, e14-, mcrA0, relA1, rpsL150(strR), spoT1, mcrB1, hsdR2*) cells unless specified otherwise. Plasmids containing wildtype *STE50* or mutants (pCW791, pCW791CC6E and pCW791CC6G) were grown overnight in Lysogeny broth (LB) liquid medium supplemented with 100 µg/µL ampicillin (LB+AMP) at 37°C with shaking at 250 rpm. The plasmids were isolated from overnight cultures using QIAGEN's QIAprep Spin Miniprep Kit. To remove the *STE50* promoter, plasmid DNA was sequentially double digested with restriction enzymes *Age*I and *Afe*I. Briefly, 3 µg of plasmid DNA was first digested with *Age*I 1X NEBuffer r1.1 at 37°C for 1-hour. Prior to the second digestion, the first buffer was removed using QIAGEN's QIAquick PCR purification kit and replaced with 1.1x Cut Smart buffer, followed by the addition of *Afe*I and incubation at 37°C for 1-hour. The reaction was heat inactivated at 70°C for 20 mins to be used for *in vivo* recombination (IVR), a cost and time efficient technique for cloning multiple constructs with natural and synthetic DNA fragments, to introduce the new promoters into a double digested vector[80].

For cloning the inducible promoters in front of the coding sequence of *STE50* through IVR, the promoters of *FIG2* (~1 kb) or *FUS1* (~1 kb) were polymerase chain reaction (PCR)[81] amplified by using Taq DNA polymerase with primers OCW2018 and OCW2019R or OCW2020 and

OCW2021R, respectively, using yeast genomic DNA from BY4741 *(MATa his3Δ1 leu2Δ0 met15Δ0 ura3Δ0)*[82] as the template. The PCR product was electrophoresed on a 1% agarose gel. Yeast transformation was performed using the "One-step" protocol (The Knight Lab)[83] with 10 µL of PCR amplified promoter (*FIG2p* or *FUS1p*) fragment mentioned above (0.5-1 µg) and ~1 µg of the double digested *STE50* plasmid in yeast strain YCW311 for IVR. The transformation was plated on a SD-Ura plate and incubated at 30℃ for three days. Single colonies were patched on a SD-Ura plate and verified through yeast colony PCR for successful recombinants with primers OCW2018 and OCW172R or OCW2020 and OCW172R for *FIG2p-STE50* (~1.4 kb) or *FUS1p-STE50* (~1.4 kb), respectively. Candidate recombinants were inoculated overnight in liquid SD-Ura medium and plasmid DNA was isolated using QIAGEN's QIAprep Spin Miniprep Kit following the manufacture's protocol except with a 1-hour incubation at 37℃ with Buffer P1 supplemented with 10 µg of Zymolyase. The plasmid DNA was eluted into 50 µL of elution buffer, and 3 µL was used for *E. coli* transformation and selection on LB+AMP at 37℃ overnight. Single colonies were inoculated in LB+AMP at 37℃ overnight and the plasmid constructs were isolated using QIAGEN's QIAprep Spin Miniprep Kit. Candidate plasmids constructs were confirmed by Sanger sequencing. All the strains, plasmids, primers, and PCR conditions can be found in Appendix A Table A1, A2, A3 and A4, respectively.

2.1.2 Construction of *STE5* Plasmids with *FIG2* Promoter

The coding sequences of the *STE5* gene and the *FIG2* promoter (~1 kb) were amplified from yeast genomic DNA of BY4741[82] using Q5 High fidelity DNA Polymerase (New England BioLabs) and primers OST003 and OST001R or OST007 and OST005R, respectively. The two products were joined using overlapping extension PCR[81,84] with primers OST007 and OST001R

with Q5 High fidelity DNA Polymerase. The plasmid backbone (p416*GAL1*) was double digested with *Xba*I and *Sac*I at 37℃ for 2-hours. The reaction was heat inactivated for 20 mins at 70℃. The products were separated on a 1% agarose gel for 1-hour and the fragment corresponding to doubly digested vector backbone was excised and gel purified using the QIAGEN QIAquick Gel Extraction Kit. Both the double digested plasmid (~1 µg) and 10 µL of the *FIG2p-STE5* (~4.0 kb) PCR products (0.5-1 µg) were used to transform yeast YCW311 (*ste50Δ::TRP1 sst2::ura3 FUS1-HIS3)* using the "One-step" Protocol[83]. Transformants were plated on SD-Ura plates and incubated at 30℃ for three days. Single colonies were picked and inoculated in 5 mL liquid SD-Ura medium for overnight culture at 30℃ with shaking at 250 rpm. Plasmid constructs were isolated from yeast YCW311 and transformed into *E. coli* using the protocol as described previously for the Ste50 plasmids. Single colonies were picked to inoculate into liquid LB+AMP grown at 37°C overnight with shaking at 250 rpm, and plasmid DNA was isolated using QIAGEN's QIAprep Spin Miniprep Kit. The p416*GAL1_FIG2p-STE5* (~9.0 kb) constructs were verified using single digestion with restriction enzymes *Xba*I and *Xho*I.

To construct *FIG2p-STE5* with the *LEU2* selection marker, 3 µg of the p415*GAL1* vector was digested with restriction enzymes *Sac*I and *Xma*I to remove the *GAL1* promoter and 3 µg of the p416*GAL1_FIG2p-STE5* (~9.0 kb) was digested with restriction enzymes *Sac*I and *Xma*I to release the *FIG2p-STE5* fragment (~3.9 kb). Both digestions were heat inactivated at 70°C and electrophoresed on a 1% agarose gel for 1-hour. The p415*GAL1* vector fragment (~6.2 kb) and the *FIG2p-STE5* (~3.9 kb) fragment were excised and purified from the gel using QIAGEN QIAquick Gel Extraction Kit. Ligation was done with T4 DNA ligase (NEB) in final volume of 20 µL consisting of 2 µL of 10x Ligase buffer, 0.5 µL of Ligase (400 000 units/mL), ~200 ng of plasmid backbone and ~250 ng of insert with incubation at 16℃ for 0.5 mins followed by 25℃ for 0.5

mins. The ligation reaction (~8 μL) was used to transform competent *E. coli* MC1061, and the transformation was plated on LB+AMP and incubated at 37℃ overnight. Single colonies were inoculated in liquid LB+AMP at 37°C overnight with shaking at 250 rpm. Plasmid DNA was isolated using QIAGEN's QIAprep Spin Miniprep Kit. The p415*GAL1_FIG2p-STE5* (~10.0 kb) constructs were verified using single digestion with restriction enzyme *Xma*I. All the strains, plasmids, primers, and PCR conditions can be found in Appendix A Table A1, A2, A3 and A4, respectively.

2.2 Functionality Test of *STE50* and *STE5* Constructs Using Transcriptional Activation Reporter Assay

Transcriptional activation reporter assays were used for functionality tests for all *GAL1p*, *FIG2p*, and *FUS1p* driven *STE50* wildtype and mutant constructs in the yeast strain YCW311 *(ste50Δ::TRP1 sst2::ura3 FUS1-HIS3)*. Plasmids were transformed into the strain using the "One-step" yeast transformation protocol[83]. Vector plasmid p416*GAL1* was used as the negative control plasmid. The transformation was plated on an SD-Ura plate at 30℃ for three days. Single colonies were then picked and patched on a SD-Ura plate, incubated at 30℃ for two days before being replicated onto SD-Ura-His plates containing various concentrations (0-100 mM) of 3-AT. The replica plates were incubated at 30℃ for three days. Similarly, functionality tests were done with p416*GAL1_FIG2p-STE5* and p416*GAL1_FUS1p-STE5* in yeast strain YCW1620 (*W303-1A, ste5Δ::hisG FUS1-HIS3, his3 leu2 trp1 ura3)*. All the strains, plasmids, primers, and PCR conditions can be found in Appendix A Table A1, A2, A3 and A4, respectively.

2.3 Gene Editing using CRISPR/Cas9

Gene editing was done in this study to delete the coding sequences of *SST1* and *FAR1* and for *HIS3* reporter integration using CRISPR/Cas9. CRISPR/Cas9 is a simple gene editing technique that requires the Cas9 protein and a small guide RNA[85–88]. The Cas9 protein gets activated in the presence of its gRNA forming a Cas9-gRNA complex and targets its protospacer adjacent motif (PAM) sequence[87]. Once bound a double standard break will occur at the targeted site leading to two different options in terms of repair, non-homologous end joining (NHEJ) or homology-directed repair (HDR)[87,89]. NHEJ is common to heterogeneous pools of insertions and deletions, resulting in a highly error prone technique when compared to HDR[89]. HDR is precise and would be the favored of the two techniques as it utilizes a homologous donor DNA that contains the two homologous regions that flank the gene cut site, allowing the repair to be done with few errors.

2.3.1 Construction of gRNA/Cas9 Plasmids for Gene Editing

Plasmids encoding gRNAs used for CRISPR/Cas9 gene editing in this study were constructed with vector plasmid pML104 (*URA3* maker) or pML107 (*LEU2* marker)[88,90,91]. The vector plasmids were obtained from Addgene, and the design and cloning of the gRNA were done as previously described[88]. All the plasmids along with the gRNA targeting sites are listed in Appendix A Table A2.

2.3.2 *SST1* and *FAR1* Deletion in YCW311 and *HIS3* Reporter Integration in YCW2405

To delete of the coding sequences of *SST1* or *FAR1*, repair template fragments were constructed by PCR using 1 μM of template strand, OCW2062 for *SST1* or OCW2063 for *FAR1*

and 10 μM of flanking primers OCW1613 and OCW1614R for *SST1* or OCW2064 and OCW2065R for *FAR1*, to facilitate HDR in CRISPR/Cas9 gene editing[89]. Reactions were carried out in a final volume of 25 μL consisting of 0.5 μL of 1 μM template strand, 0.5 μL of 10 μM of each primer, 2 μL dNTP mix each at 2.5 mM, 2.5 μL of 10x Taq Buffer (500 mM KCl, 200 mM Tris-HCl (pH 8.4), 15 mM $MgCl_2$), 0.25 μL of 10 U/μL of Taq polymerase and 18.75 μL of dH_2O. Following the PCR reaction, 10 μL of 0.5-1 μg PCR product was used to transform yeast strain YCW311 using the "One-step" yeast transformation protocol[83] along with two gRNA/Cas9 plasmids (~2 μg) pCW1500 and pCW1512 for *SST1* or pCW1683 and pCW1689 for *FAR1*. Transformed cells were plated on SD-Ura-Leu plates and incubated at 30℃ for three days before single colonies were picked and verified using yeast colony PCR with primers OCW2085 and OCW2086R for *SST1* or OCW957 and OCW958R for *FAR1*. The PCR reaction was carried out in a final volume of 25 μL consisting of 3 μL of cell lysate (a yeast colony in 20 μL of lysis buffer (20 mM NaOH, 0.1 mg/mL RNase A)) as template, 0.5 μL of 10 μM of each primer, 2 μL of dNTP mix each at 2.5 mM, 2.5 μL of 10x Taq Buffer, 0.25 μL of 10 U/μL Taq polymerase and 16.25 μL of dH_2O. These gene editing manipulations resulted in the following strains: YST100 (YCW311 *sst1Δ*), YST200 (YCW311 *far1Δ*) and YST300 (YCW311 *sst1Δ far1Δ)*

To construct yeast strains with the *HIS3* reporter gene under different pheromone inducible promoters, YCW2405 (yWS677 (BY4741 *sst2Δ far1Δ bar1Δ ste2Δ ste12Δ gpa1Δ ste3Δ mf(alpha)1Δ mf(alpha)2Δ mfaΔ mfa2Δ gpr1Δ gpa2Δ) STE2, GPA1 STE12* derivative was used as the starting strain[65]. The *HIS3* gene was integrated at the *FUS1*, *FIG1* or *FIG2* locus under the respective promoter using CRISPR/Cas9 gene editing. This was done by co-transforming YCW2405 using *HIS3* with both 5'- and 3'- flanking sequences of the locus to be integrated along with two gRNA/Cas9 plasmids targeting both N- and C-terminal sites of the coding sequence of

the targeted locus: pCW1691 and pCW1693 targeting *FUS1*; pCW1695 and pCW1697 targeting *FIG1*; pCW1699 and pCW1701 targeting *FIG2*. Edited candidates were identified and verified by yeast colony PCR, reporter function analysis, and Sanger sequencing. The gene editing manipulation resulted in the following *HIS3* reporter bearing strains: YCW2432 (YCW2405 *FUS1p-HIS3*), YCW2433 (YCW2405 *FIG1p-HIS3*) and YCW2434 (YCW2405 *FIG2p-HIS3*). All the strains, plasmids, primers, and PCR conditions can be found in Appendix A Table A1, A2, A3 and A4, respectively.

2.4 Functionality Characterization of Gene Edited Strains

The strains that had undergone gene editing were tested through different assays to ensure that they have either lost or gained the genes functionality. A barrier assay was performed for *SST1/BAR1* functionality, and a halo assay was done for *FAR1* functionality[59,92]. As for the *HIS3* functionality a reporter assay was done using transcriptional activation as described in section 2.5.1 and 2.5.2.

2.4.1 Barrier Assay for *SST1/BAR1* Functionality

The barrier assay consists of testing the strain to establish if it can produce the protease to cleave α-factor[92]. A streak of *MAT*α cells as the source of α-factor can cause cell cycle arrest of the lawn of supersensitive *MAT***a** cells forming a clear, no-growth zone. In the assay the strains to be tested were streaked as thin lines parallel to and in the vicinity of the *MAT*α cells. Cells that are wild type at the *SST1* locus release the protease and thus degrade the α-factor and prevent it from crossing the streak of cells and causing cell cycle arrest in the tester lawn cells beyond it. If cells

are *sst1Δ*, no protease is produced, the α-factor can diffuse freely across the line of cells being tested and is able to cause cell cycle arrest in cells of the tester lawn beyond the streak.

The barrier assay was performed as described[92]. Briefly, 1 mL of overnight culture of YCW321 *MAT***a** strain was mixed with 4 mL of dH_2O and 50 µL of this dilution was plated on a YPD plate and let dry for 15 mins. Once dry, a fine line of YCW57 *Matα his1* strain was spread on the middle of the plate. Around the *Matα* strain were spread fine lines of the strains to be tested for *SST1* functionality. Once complete, plates were incubated for two days at 30°C. YCW2052 was used as a positive control (*SST1*) and YCW1886 was used as a negative control (*sst1Δ*).

2.4.2 Halo Assay for *FAR1* Functionality

The halo assay is used to test the status of the *FAR1* gene by measuring the cells' ability to undergo cell cycle arrest in response to pheromone. A lawn of cells of the strain being tested is introduced to the α-factor[59]. Those that are *FAR1* will experience cell cycle arrest forming a clear (no growth) zone when enough α-factor is present; those that are *far1Δ* will not exhibit cell cycle arrest even in the presence of α-factor and no growth inhibition zone will be observed[59].

Halo assays were performed as described[40]. Briefly, 0.5 OD_{600} of cells from an overnight culture in appropriate medium were mixed into 6 mL of appropriate medium containing 2 % molten agarose (cooled to ~56°C) and plated over pre-warmed (37°C) plates of appropriate medium. Plates were left to solidify for 15 mins before spotting with 2 µL of α-factor (500, 50, 5, 0.5 µM). Plates are incubated at 30°C for two to three days before scoring.

2.5 Transcriptional Activation Reporter Assays

Ligand-mediated signaling can be determined using different reporter assays measuring the pheromone pathway activities, allowing us to utilize strains with integrated reporter genes. The reporter gene is usually chromosomally integrated into strains under the control of an inducible promoter that is activated by Ste12 inside the nucleus of the cells. The two reporters that are used for this project include the yeast *HIS3* gene and GFP that can be verified through different transcriptional activation assays or GFP fluorescence assays, respectively. Strains containing the *HIS3* gene can be used to test for growth on histidine-deficient medium containing various concentrations of 3-amino-1,2,4-triazole (3-AT), a competitive inhibitor of the *HIS3* gene product, for graded selection for different strengths of reporter activities[93,94]. This can be used to screen out strains that contain some form of background activation (allowing real positives to be identified)[94]. GFP is a highly stable fluorescent protein that can be monitored using fluorescence-assaying instruments[95]. It has an excitation wavelength at 488 nm and an emission wavelength at 509 nm that can be easily detected using a flow cytometer[96]. Flow cytometry is a powerful technique used in multiple fields of life science research and is used to analyze single cells or particles as they flow past a single laser[97]. Cells expressing GFP will be detected, allowing us to determine the activity of the reporter in the presence of a ligand at different concentrations and at different time intervals.

2.5.1 Transcriptional Activation Assay of *HIS3* Reporter

For transcriptional activation assays using yeast strains with the *HIS3* reporter, yeast cells were grown in YPD medium overnight in a 30°C incubator with shaking at 250 rpm. An equivalent of 1.5 OD_{600} was centrifuged at 13 000 rpm and resuspended in 300 µL of dH_2O. Of this

resuspension, 2 µL (~100 000 cells) were mixed with 2 µL of dH_2O and spotted on SD-His plate containing 0-100 mM 3-AT in triplicate with no α-factor. The plates were incubated at 30℃ for three days and cell growth was scored to determine the baseline for cell growth in the absence of α-factor. Once the baseline is determined a similar test is done with the replacement of 2 µL of dH_2O with 2 µL of 5.6 µM alpha factor. Plates are then incubated at 30℃ for three days. The α-factor treatment allows us to determine if the cells can produce more histidine through transcriptional activation allowing cells to grow at higher concentration of 3-AT. Plasmid constructs were transformed into the strain (YCW2433 (YCW2405 *FIG1p-HIS3*)) and retested for new basal levels on SD-Ura-Leu-His plates containing 0-100 mM 3-AT in duplicate with no α-factor and incubated at 30℃ for three days. Plates were scored again to verify plasmid selection and transcriptional activity of the strain with the constructs.

2.5.2 Reverse Halo Assay of Transcriptional Activation of *HIS3* Reporter

Once the baseline was obtained for cell growth with constructs designed for the positive feedback loops, a reverse halo assay is done to compare the cell's ability to grow at different concentrations of α-factor. SD-Ura-Leu-His plates containing 5 mM or 10 mM 3-AT were made for this assay as no growth was observed at these concentrations in the absence of α-factor. Cells were grown overnight in liquid SD-Ura-Leu medium at 30°C with shaking at 250 rpm. An equivalent of 0.5 OD_{600} of cells was mixed into 6 mL of SD-Ura-Leu-His with either 5 mM or 10 mM of 3-AT and molten agarose cooled to ~56°C. The mixture is quickly vortexed and poured over the SD-Ura-Leu-His plates containing either 5 mM or 10 mM 3-AT. Plates were left to solidify for 15 mins before 2 µL of different concentrations of α-factor (560 nM, 280 nM, 140 nM,

70 nM and 35 nM) were spotted. Plates were incubated at 30°C for two days and scored for the zones of cell growth.

2.5.3 GFP Reporter Fluorescence Assay

Yeast cells (YCW2418 (WCY67, (melatonin biosensor) BY4741 *fig1Δ::ENVY(gfp) sst2Δ ste2Δ GPA1(468-472Δ)-GNAI3(350-354)[EF]::PGK1p-MTNR1A-TDH1*)[98]) were grown overnight in YPD at 30°C with shaking at 250 rpm[98]. The cells were transformed using the "One-step" Protocol for Transforming Yeast[83] with plasmid constructs and plated on SD-Ura-Leu plates. The plates were then incubated at 30°C for three days. Single colonies were grown in 5 mL liquid SD-Ura-Leu medium over four days at 30°C with shaking at 250 rpm. On day four, cells with an OD_{600} of 2 were split into eight different Falcon tubes and were introduced to 1 mL of SD-Ura-Leu containing 0, 0.01, 0.05, 0.025, 1, 5, 25 or 100 μM melatonin. The Falcon tubes were placed in a 30°C incubator with shaking at 250 rpm for 4-hours and 100 μL was transferred into a 96 well plate in triplicate after mixing with 50 μL of 0.01 M Phosphate-Buffered Saline (PBS) (0.138 M NaCl; KCl - 0.0027 M, pH 7.4 at 25°C). The 96 well plate was analyzed for GFP fluorescence using flow cytometer (BD LSRFortessa™ Cell Analyzer). A gate was set to differentiate the positive GFP cells from the negative GFP cells using the unstimulated YCW2418 strain with Vec1/Vec2 setup at time 0. All fluorescence measurements past the gate were considered as real positive GFP cells to be later used to calculate the fluorescence index. Cells were excited at 488 nm and then fluorescence was measured at 530 nm with a 30 nm gate. Measurements were taken in triplicate and the mean GFP fluorescence was multiplied by the percentage of positive GFP cells to calculate the average fluorescence index and the standard deviation at each concentration. The results were plotted on a bar graph using Microsoft Excel and the P-values obtain from the t-test:

paired two sample for means for every feedback loop setup in comparison to the control and the single feedback loops in comparison to the dual feedback loop was also included in the graph. The relative effects of every feedback loop in comparison to the control along with the standard deviation was calculated at every concentration > 0.05 μM and plotted on a bar plot using Microsoft Excel. The P-values of the single feedback loops in comparison to the dual feedback loop was calculated as previously described and was included on the bar plot. The calculated average fluorescence index, ratios and P-values can be found in the Appendix A Table A5, A7 and A6 or A8, respectively.

CHAPTER 3: RESULTS

3.1 Strain Selection for Transcriptional Assay with *HIS3* Reporter

For the transcriptional activation of the *HIS3* reporter gene we selected a few strains to test. Initially, we tested YCW311 (*MAT**a** ste50Δ::TRP1 sst2::ura3 FUS1-HIS3*) which contained the *STE50* knockout. However, as this strain contained *SST1* and *FAR1* and with previous work demonstrating that the removal of these genes is beneficial for transcriptional activation, we performed knockouts of these genes to create new strains, YST100 (YCW311 *sst1Δ*), YST200 (YCW311 *far1Δ*) and YST300 (YCW311 *sst1Δ far1Δ*). All the strains were verified through colony PCR and tested for *SST1* and *FAR1* functionality using the barrier assay (**Fig 7**) and the halo assay (**Fig 8**), respectively. These strains were very useful in testing the function of Ste50 during the study due to its *ste50* deletion (**Fig 9**).

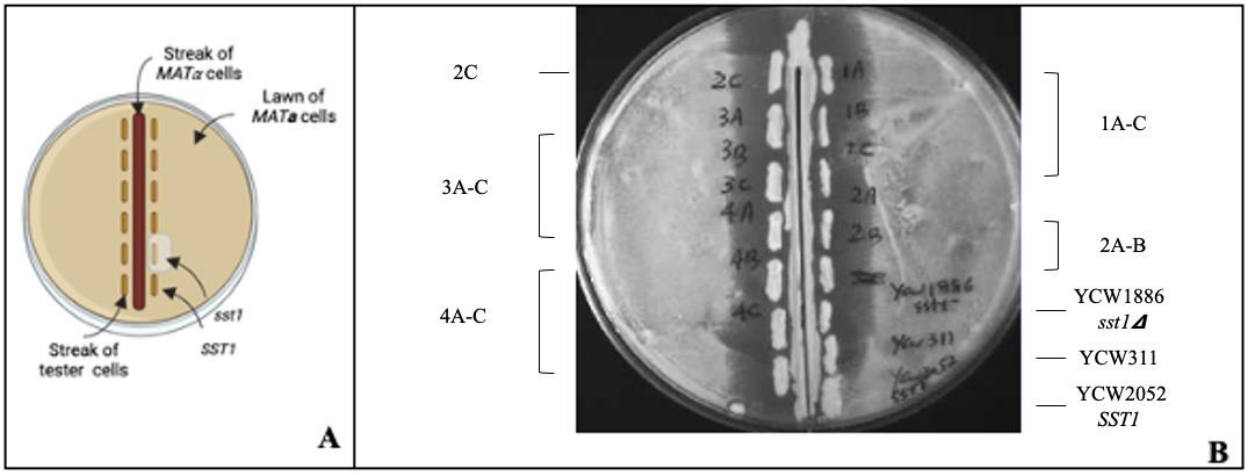

Figure 7. Barrier assay to test for *SST1* function. Figure 1A represents the schematic representation of the barrier assay. Cells that are *SST1* will not form a clear patch of cells due to the presence of the protease that degrades pheromone released from the *MATα* strain. Figure 1B represents the barrier assay done on the tester cells from YST100 strain with *sst1Δ* derived from YCW311. Tester cells 1A to 4C confirm *sst1Δ* due to the α-factor from YCW57 *MATα* strain crossing the tester cells arresting YCW321 *MAT**a*** strain. Strains YCW2052 and YCW1886 were used as positive and negative controls, respectively.

Halo assay Schematic	Strains tested	*STE50* Plasmid	Vec Plasmid
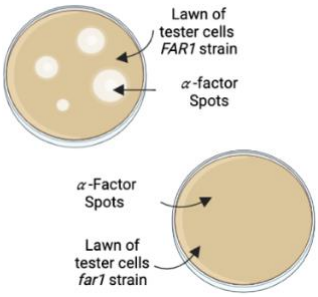	YCW311 *ste50Δ::TRP1 sst2::ura3 FUS1-HIS3* (+ control)	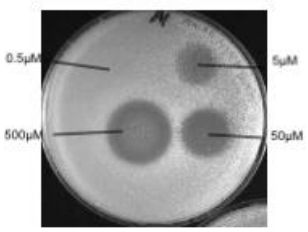 **A**	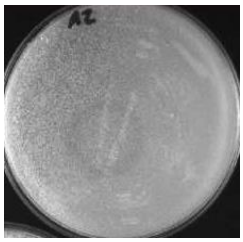 **E**
	YCW100 *ste50Δ::TRP1 sst2::ura3 sst1Δ FUS1-HIS3*	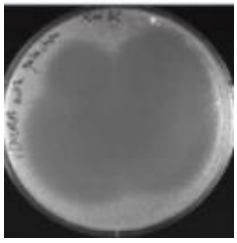 **B**	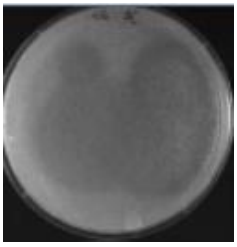 **F**
	YST200 *ste50Δ::TRP1 sst2::ura3 far1Δ FUS1-HIS3*	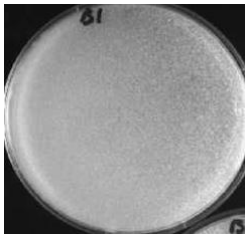 **C**	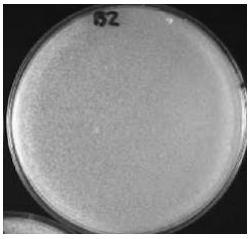 **G**
	YST300 *ste50Δ::TRP1 sst2::ura3 sst1Δ far1Δ FUS1-HIS3*	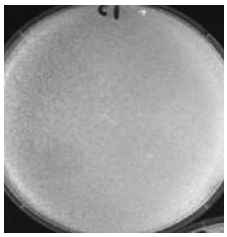 **D**	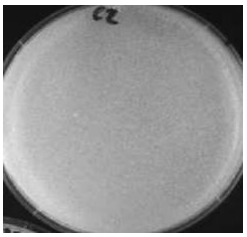 **H**

Figure 8. Halo assay to test for *FAR1* function. First column represents the schematic of the halo assay. Strain for *FAR1* will form a clear patch in the presence of α-factor as cell are capable of mediating cell cycle arrest whereas cells for *far1Δ* will not. Second column represents different strains tested for *FAR1* activity, YCW311 (8A and E), YST100 (8B and F), YST200 (8C and G) and YST300 (8D and H). The third and fourth column represents the plasmids that were transformed into each tested strain in column two with pCW791(*STE50*) and p416*GAL1* (Vec), respectively. Cells were spotted with 500 μM, 50 μM, 5 μM and 0.5 μM of α-factor. YCW311 were used as positive control. YST200 and YST300 confirm *far1Δ*.

The barrier assay confirms the knockout of *SST1* in several colonies that were obtained after performing gene editing on YCW311 using CRISPR/Cas9 creating the new YST100 strain (**Fig 7B**). As seen in figure 7B the different tester cells of 1A-C, 2A-C, 3A-C and 4A-C are all able to form a clear "no growth" patch on the YCW321 *MAT**a*** strain similar to the YCW1886 that was used as a negative control. This indicates that the α-factor was able to cross those mentioned strains and cause the cell cycle arrest in the hypersensitive YCW321 *MAT**a*** strain. YCW311 and YCW2052 containing *SST1* successfully prevented the α-factor from YCW57 *MATα* strain from crossing and arresting YCW321 *MAT**a*** strain to grow freely beyond the spread of the cells (**Fig 7B**). Halo assays confirm the knockout of *FAR1* for YST200 and YST300 derived from YCW311 and YCW100, respectively (**Fig 8**). In response to α-factor YST200 and YST300 failed to arrest when compared to YCW311 and YST100, in the presence of the *STE50* vector (**Compare C and D to A and B in Fig 8**). In the absence of *STE50,* pheromone induced cell cycle arrest signaling is still capable of going through, but generates a much weaker response as the halo fails to form as intensely as when a *STE50* plasmid is present (**Compare E to A and F to B in Fig 8)**.

We also created new yeast strains derived from yWS677 (BY4741 *sst2Δ far1Δ bar1Δ ste2 Δ ste12Δ gpa1Δ ste3Δ mf(alpha)1Δ mf(alpha)2Δ mfa1Δ mfa2Δ gpr1Δ gpa2Δ) STE2, GPA1 STE12*, as YCW2405) using CRISPR/Cas9 gene editing[65]. The resulting strains have the *HIS3* reporter under different pheromone inducible promoters, YCW2432 (YCW2405 *FUS1p-HIS3*), YCW2433 (YCW2405 *FIG1p-HIS3*) and YCW2434 (YCW2405 *FIG2p-HIS3*). These strains were used to perform the spotting assay to determine which of the promoters had a lower basal level in the absence of pheromone, and to verify its ability to activate transcription to produce His3 to be tested in the reverse halo assay to observe the long-term effect of overproducing Ste50, Ste5 or Ste50 and Ste5 through the controlled feedback loop.

3.2 Transcriptional Activation Assays with *HIS3* Reporter

3.2.1 Spotting Assay on YCW311 and Derivatives to Recapitulate the Effects of *SST1* and *FAR1* Knockouts on the Pheromone Response Pathway.

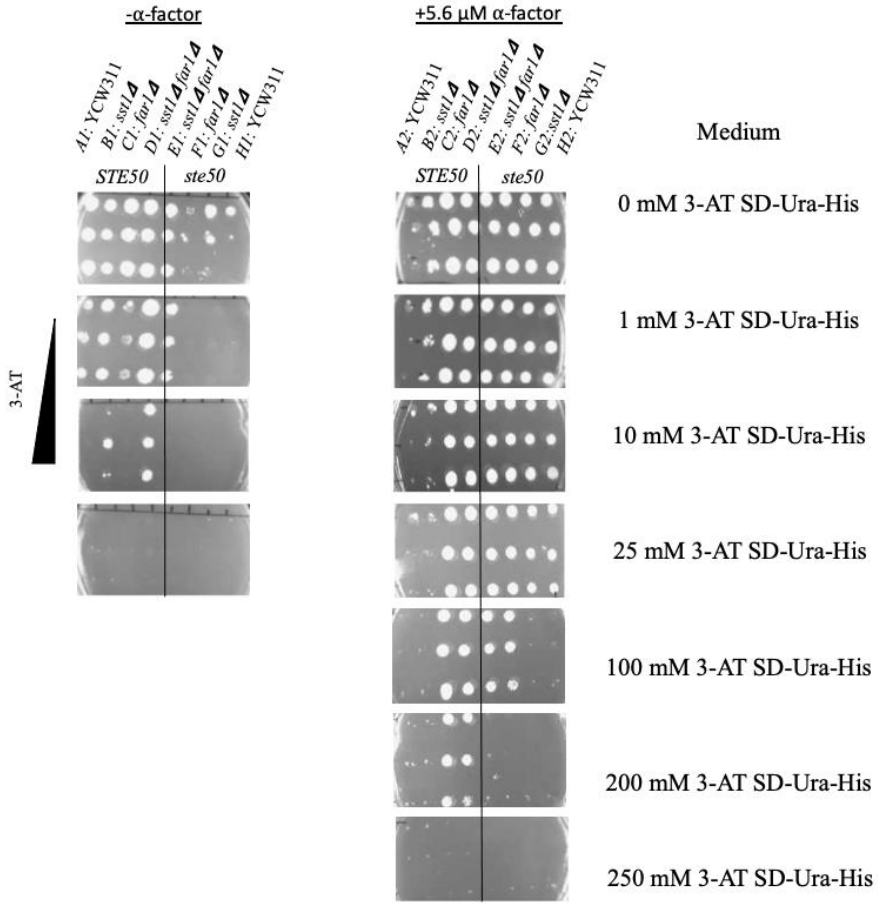

Figure 9. Spotting assay with YCW311, YST100, YST200 and YST300 in the absence and presence of *α*-factor. Transcriptional activation of *HIS3* through a spotting assay with 100 000 cells of YCW311 **(***MATa ste50Δ::TRP1 sst2::ura3)* and its derivatives: YST100 (*sst1Δ)*, YST200 (*far1Δ)* and YST300 (*sst1Δfar1Δ*) in the absence and presence of *α*-factor (5.6 μM). A control vector was used to observe the flow of signal in the absence of *ste50* and a *STE50* plasmid on its own promoter was used to demonstrate the importance of *STE50* for the pheromone pathway.

Transcriptional activation measured through a spotting assay was done here with YCW311 and its derivatives to determine the basal levels of each of the strains and to observe the effects the *sst1Δ far1Δ* had on the transcriptional activation of *HIS3* by the pheromone pathway. In the absence of pheromone and with the *STE50* construct all the strains can grow on SD-Ura-His

medium containing 1 mM 3-AT (**See A1-D1 in Fig 9**), whereas with the control vector (no Ste50 present in the cells), they are able to grow on 0 mM 3-AT SD-Ura-His demonstrating the low basal level (**See E1-H1 in Fig 9**). In the stimulated state with 5.6 μM of α-factor, YST300 (*sst1Δ far1Δ)* and YST200 *(far1Δ)* can grow on higher concentration of 3-AT when compared to YCW311 and YST100 (*sst1Δ)* regardless of the Ste50 state (**Compare C2, D2, E2 and F2 with A2, B2, G2 and H2 in Fig 9**), emphasizing the importance of *FAR1* deletion for proper transcriptional activation reporter assays**.** The importance of *sst1Δ* is harder to observe in this assay due to immediate cell cycle arrest in the presence of high levels of α-factor with the functional *STE50* plasmid when comparing YST100 (*sst1Δ)* to YCW311 (**See A2 and B2 in Fig 9**). However, the importance of *STE50* can be seen, where in the absence of Ste50 with the control vector YST100 and YCW311 are able to grow at higher concentration of 3-AT as there is a weaker flow of signal to activate *FAR1* allowing the cells to produce necessary His3p to grow at higher concentrations of 3-AT (**See G2 and H2 in Fig 9**). As these strains all were *ste50Δ* we switched to the YCW2405 derived strains to test what would happen if we had additional copies of *STE50* and *STE5* as it had all the necessary components of the pheromone pathway.

3.2.2 Spotting Assay on YCW2405 and Derivatives to Assess the Basal and Stimulated Transcriptional Activity of the *HIS3* Reporter

A spotting assay was performed using synthetic dextrose (SD) as the control plate and SD-His plates with different concentrations of 3-AT for any reporter activity in the absence of α-factor. Strains tested here were the YCW2405 (no reporter) and its derivatives YCW2432 (YCW2405 *FUS1p-HIS3*), YCW2433 (YCW2405 *FIG1p-HIS3*) and YCW2434 (YCW2405 *FIG2p-HIS3*) to examine which of the three promoter-reporters had the lowest basal activity. Each of the derivatives had different basal levels of reporter activity. Strains YCW2432, YCW2433, and

YCW2434 were capable of growing on, respectively, 1 mM 3-AT SD-His, 0 mM 3-AT SD and 0 mM 3-AT SD-His, respectively in the absence of α-factor demonstrating that YCW2433 had the lowest basal activity (**See B1, C1 and D1 in Fig 10**). To test each strain's reporter activity to ensure that they had the ability to produce His3p for the reverse halo assay, another spotting assay was performed using 2 µL of 5.6 µM of α-factor instead of dH_2O on similar plates. Results show that in the presence of α-factor, all the derivatives of YCW2405 could grow in selective medium with high concentrations of 3-AT (**See B2, C2 and D2 in Fig 10**).

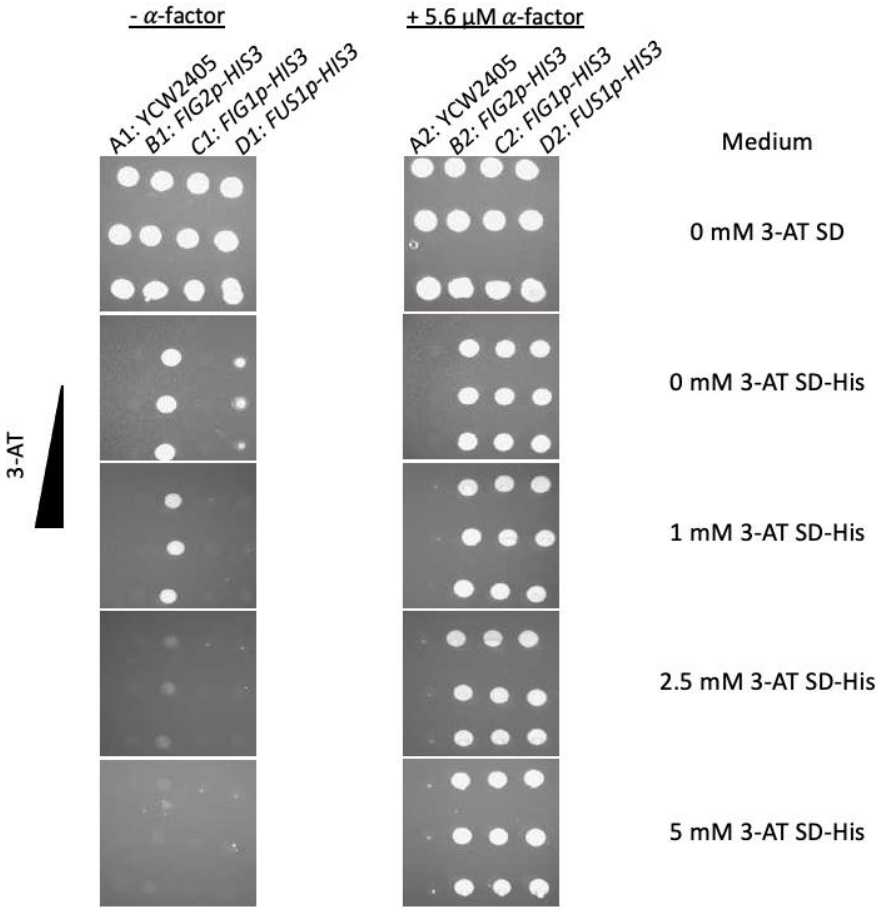

Figure 10. Spotting assay with YCW2405 and its derivatives YCW2432 (*FUS1p-HIS3*), YCW2433 (*FIG1p-HIS3*) and YCW2434 (*FIG2p-HIS3*) in the absence and presence of α-factor. Spotting assay to observe the basal level of reporter activity of each strain as titrated at different concentrations of (0-5 mM) 3-AT and to compare the different basal levels of each *HIS3* reporter. Spotting assay was done in triplicate with ~100 000 cells at each spot with either 2 µL of dH_2O or 2 µL of α-factor at 5.6 µM.

3.2.3 Spotting Assay with YCW2433 with my *STE50* and *STE5* Constructs to Obtain the Conditions for the Reverse Halo Assay

To compare the feedback loop system, we transformed a two-plasmid system in the following combinations, as control Vec (*URA3*) with a Vec (*LEU2*), Vec (*URA3*) with *pFIG2p-STE5 (LEU2)* to produce Ste5, *pFUS1p-STE50 (URA3)* with the Vec (*LEU2*) to produce Ste50, and *pFIG2p-STE50 (URA3)* with the *pFIG2p-STE5 (LEU2)* to produce both Ste50 and Ste5 into YCW2433 (BY4741 *sst2Δ far1Δ bar1Δste2Δ ste12Δ gpa1Δste3Δ mf(alpha)1Δ mf(alpha)2Δ mfa1Δ mfa2Δ gpr1Δ gpa2ΔSTE2, GPA1 STE12 FIG1p-HIS3*. Spotting assays with the transformants were done on SD-Ura-Leu to ensure the selection of both plasmids and SD-Ura-Leu-His plates containing 0-10 mM of 3-AT to observe any transcriptional activity that might have occurred from a leaky plasmid in the two-plasmid system. Growth was only seen on 0 mM 3-AT SD-Ura-Leu indicating no detectable basal level of expression in the absence of α-factor (**Fig 11**). Using this guide the reverse halo assay was performed on SD-Ura-Leu-His plates with 5 mM or 10 mM 3-AT.

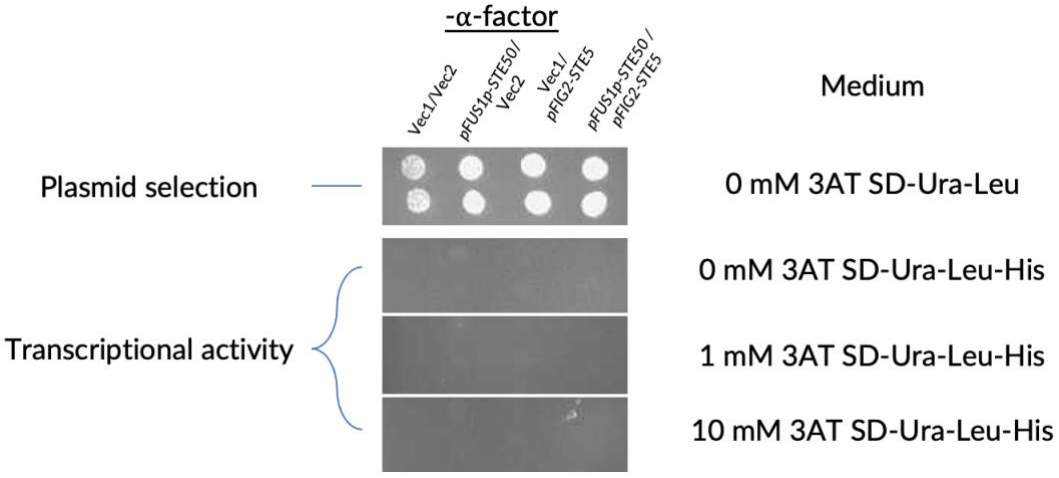

Figure 11. Spotting assay of YCW2433 (*FIG1p-HIS3*) transformants in the absence of α-factor. Vec (*URA3*)/Vec (*LEU2*), p*FUS1p-STE50* (*URA3*)/Vec (*LEU2*), Vec (*URA3*)/p*FIG2p-STE5* (*LEU2*) and p*FUS1p-STE50* (*URA3*)/p*FIG2p-STE5* (*LEU2*) were transformed into YCW2433. Spotting assay was done in duplicates with ~100 000 cells per spot. The first plate was used for plasmid selection and the histidine-deficient plates were used to observe transcriptional activity of the *HIS3* reporter.

3.2.4 Reverse Halo Assay to Observe the Long-Term Effects of *STE50* and *STE5* Upregulation

To observe the long-term effects of induced overexpression of *STE50* and *STE5* individually or in combination through the *HIS3* reporter gene, a reverse halo assay was done using YCW2433 (BY4741 *sst2Δ far1Δ bar1Δste2Δ ste12Δ gpa1Δste3Δ mf(alpha)1Δ mf(alpha)2Δ mfa1Δ mfa2Δ gpr1Δ gpa2Δ STE2, GPA1 STE12 FIG1p-HIS3)* with the two-plasmid system mentioned in section 3.2.3. The layout for the reverse halo assay of the different concentrations of α-factor can be seen in figure 12.

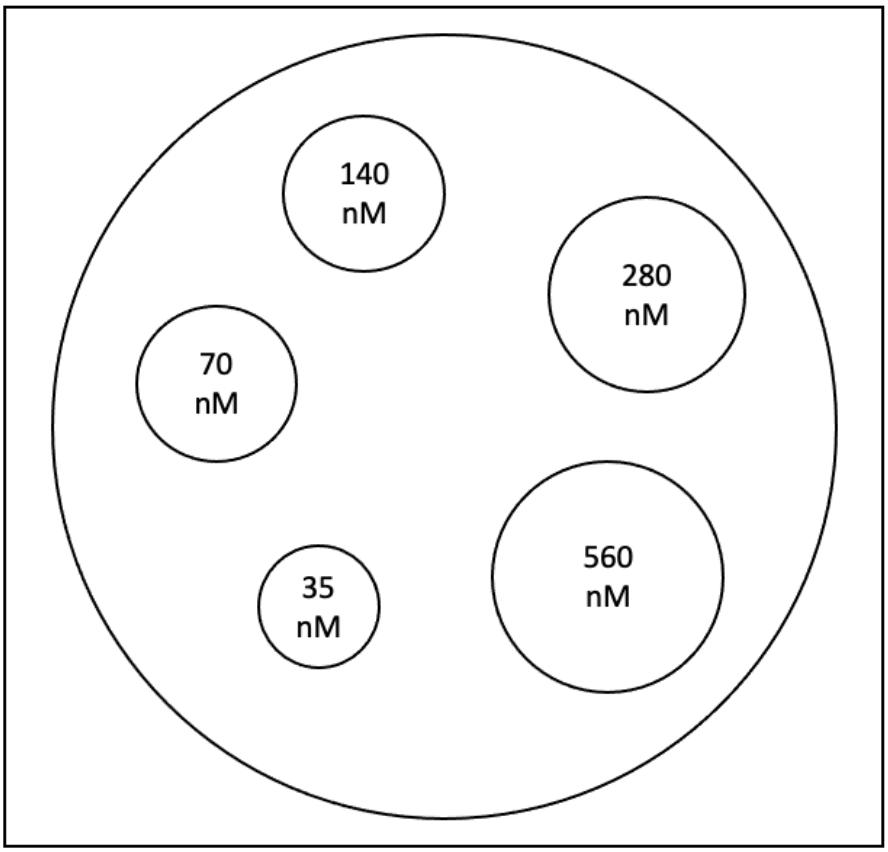

Figure 12. Layout diagram of the reverse halo assay. Diagram indicating the plate position of 2 µL of each concentration of α-factor (560 nM, 280 nM, 140 nM, 70 nM, and 35 nM) was spotted on the cells being tested to observe transcriptional activation of *HIS3* reporter in YCW2433 (YCW2405 *FIG1p-HIS3)*. The general trend in response to the different concentrations of α-factor is shown.

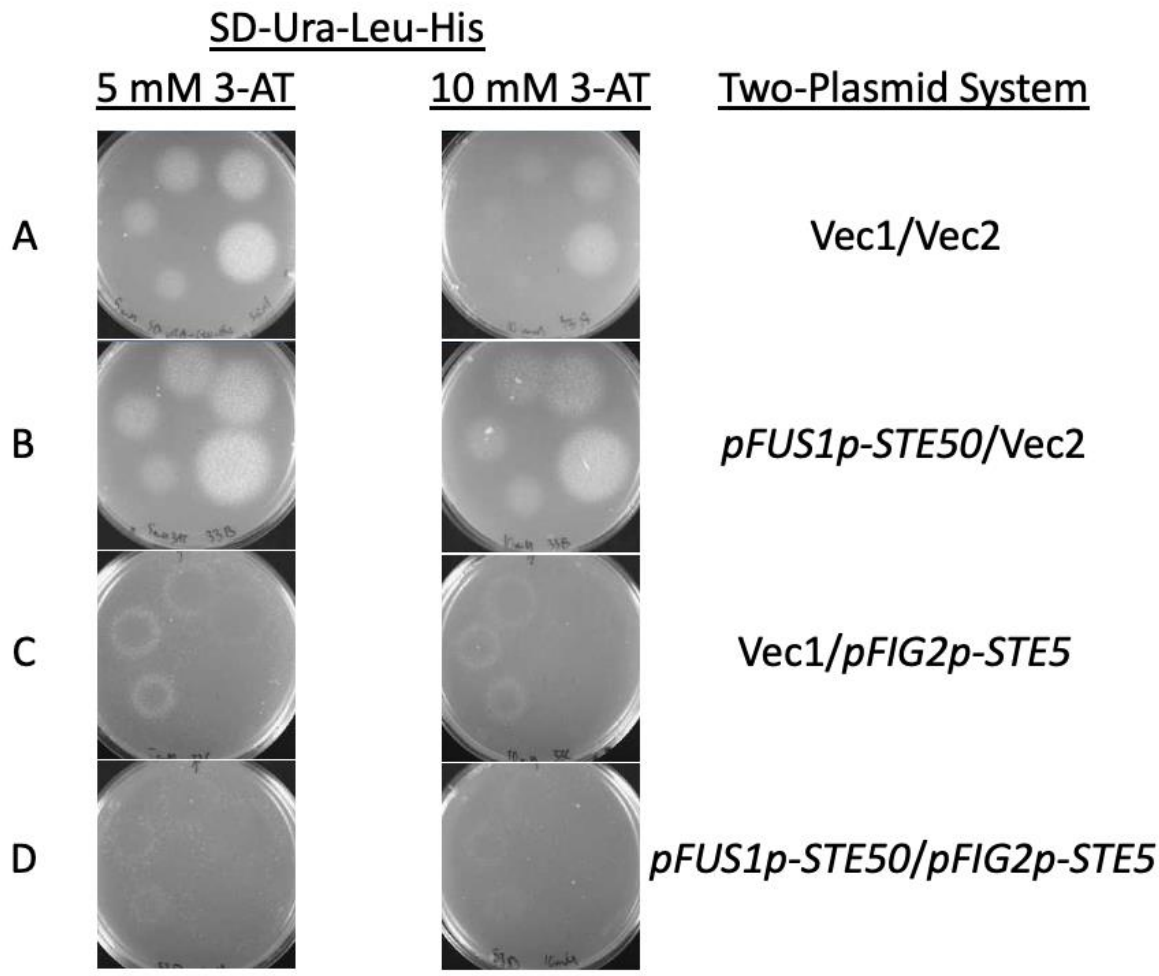

Figure 13. Reverse halo assay with YCW2433 (*FIG1p-HIS3)* transformants on SD-Ura-Leu-His with 5 mM or 10 mM 3-AT. The two-plasmid system consisting of Vec (*URA3*)/Vec (*LEU2*), p*FUS1p-STE50* (*URA3*)/Vec (*LEU2*), Vec (*URA3*)/p*FIG2p-STE5* (*LEU2*) and p*FUS1p-STE50* (*URA3*)/p*FIG2p-STE5* (*LEU2*) were transformed into YCW2433 and spotted with 2 µL of α-factor at 560 nM, 280 nM, 140 nM, 70 nM and 35 nM.

The reverse halo demonstrated that on the 5 mM 3-AT plates with more Ste50 in the cells a much larger halo of growth was seen as compared to the control at every concentration of α-factor (**Compare B with A in Fig 13**). Interestingly however, having more Ste5 and both Ste50 with Ste5 resulted in an initial greater response to α-factor followed by cell cycle arrest (**C and D in Fig 13)**. Similar results were seen at 10 mM 3-AT plates; however, the control vector is incapable of giving a response at 35 nM and 70 nM of α-factor when compared to additional Ste50 (**Compare B and A in Fig 13).**

3.3 Melatonin Biosensor Transcriptional Activation of GFP with Melatonin

To assay the relatively short-term effects of over-producing Ste50 and Ste5 individually and together, the melatonin biosensor YCW2418 (BY4741 *fig1Δ::ENVY(gfp) sst2Δ ste2Δ GPA1(468-472Δ)-GNAI3(350-354)[EF]::PGK1p-MTNR1A-TDH1*)[98] was used.

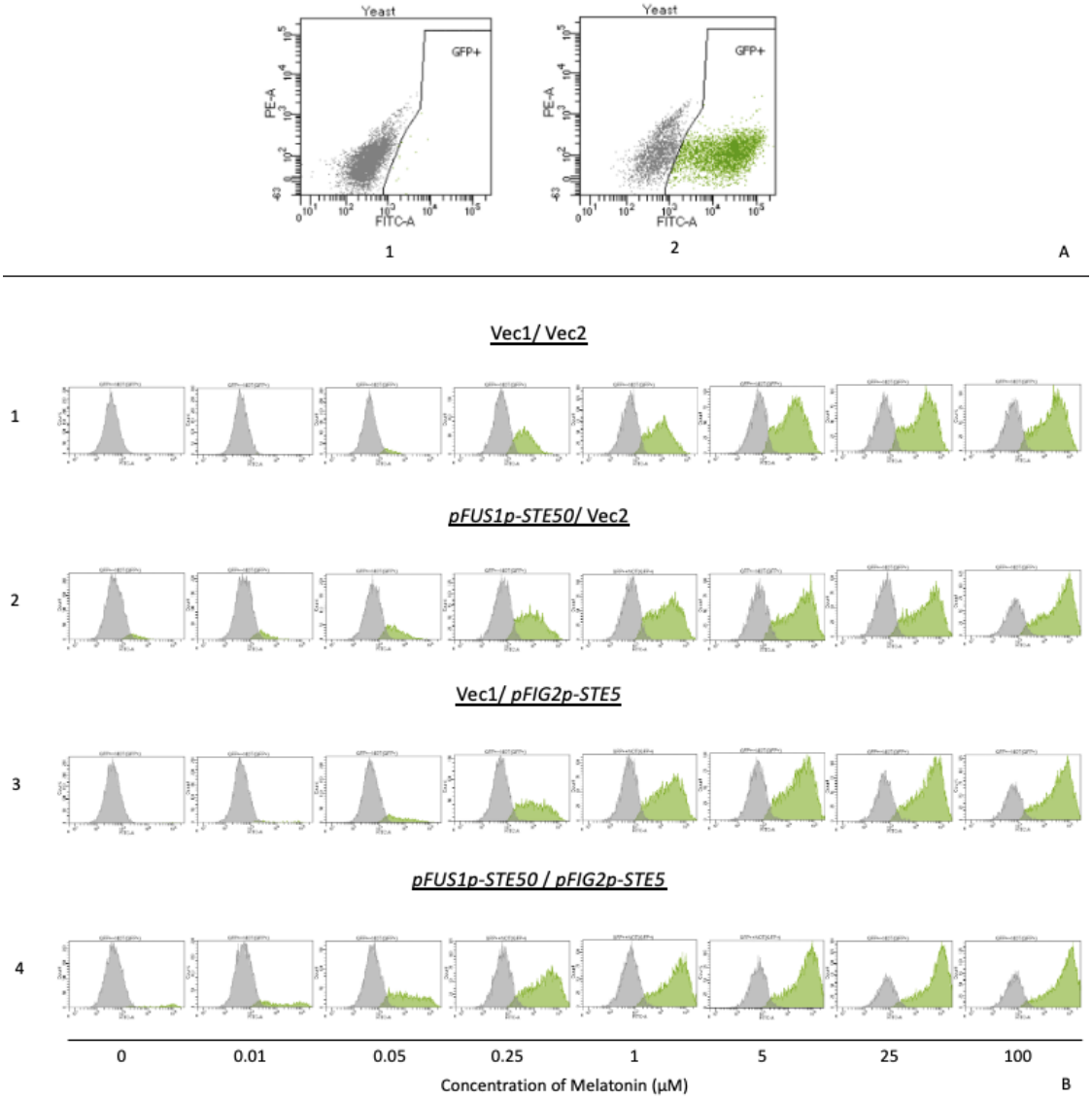

Figure 14. Cytometry analysis of the effects of the positive feedback loops on the melatonin biosensor. Section A represents the YCW2418 with Vec1/Vec2 setup in the presence of no ligand (A1) to set the gate and with 100 μM (A2) as a positive control. Section B demonstrates the change in GFP fluorescence seen for YCW2418 in the presence of the two-plasmid system, Vec1/Vec2 (B1), *pFUS1p-STE50/*Vec2 (B2), Vec1/*pFIG2p-STE5* (B3) and *pFUS1p-STE50/pFIG2-STE5* (B4) at different concentrations of melatonin after 4-hours treatment. Green area indicates GFP+ population, and grey area indicates GFP- population.

The shift in GFP fluorescence in the dual feedback loop and the single feedback loop occurs at lower concentrations of melatonin (0.05 µM) compared to the control vector at 0.25 µM (**Compare B2, B3 and B4 to B1 in Fig 14**). In addition, the shift is much more intense looking at 100 µM of melatonin with the positive feedback loops when compared to the control vector.

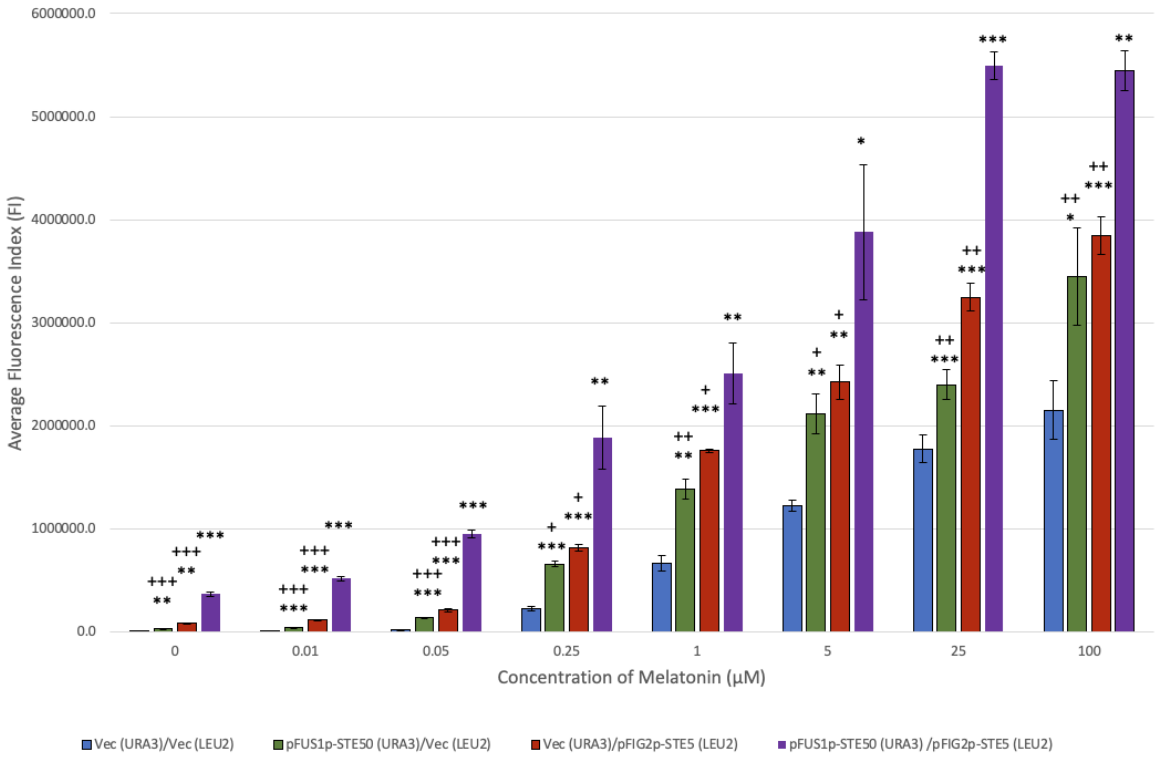

Figure 15. Effects of Ste50 and Ste5 positive feedback loops on the signaling output of the melatonin biosensor. The average mean total GFP fluorescence index of the entire population of YCW2418: (BY4741 *fig1Δ::ENVY(gfp)sst2Δ ste2Δ GPA1(468-472Δ)-GNAI3(350-354)[EF]::PGK1p-MTNR1A-TDH1*) with transformants: Vec (*URA3*)/Vec (*LEU2*) , *pFUS1p-STE50* (*URA3*)/Vec (*LEU2*), Vec (*URA3*)/*pFIG2p-STE5* (*LEU2*) and *pFUS1p-STE50* (*URA3*)/*pFIG2p-STE5* (*LEU2*) measured after 4-hours treatment with melatonin at 0 µM, 0.01µM, 0.05 µM, 0.25 µM, 1 µM, 5 µM, 25 µM, and 100 µM, and plotted on a bar graph. (*, P-values in respect to Vec1/Vec2 and +, P-values in respect to *pFUS1p-STE50*/*pFIG2p-STE5*; * or +, P < 0.05; ** or ++, P < 0.01; *** or +++ P <0.001)

We observed that having both feedback loops together and alone were better than the vector alone at every concentration of melatonin (**Compare green, red, and purple to blue in Fig 15**). The calculated P-values at every concentration for each feedback loop in comparison to the control vector is < 0.05 indicating significant difference. In addition, the dual feedback loop is also

significantly greater than either feedback loop alone with P-value < 0.05 at every concentration calculated (**Compare green and red to purple in Fig 15**).

To compare the pathway output that is influenced by the feedback loop under various dosage of ligand stimulation, we calculated the ratio of fluorescence index between each feedback loop to the vector control at every concentration of melatonin tested (**Fig 16**). Looking at the ratio of every feedback loop compared to the vector only, the melatonin pathway is more sensitive with positive feedback loops at lower concentrations of melatonin (<1 μM) compared to higher concentrations of melatonin (>1 μM) (**Fig 16**). The double feedback loop is of higher sensitivity to either feedback alone with P-values < 0.05 (**Compare green and red to purple in Fig 16**)

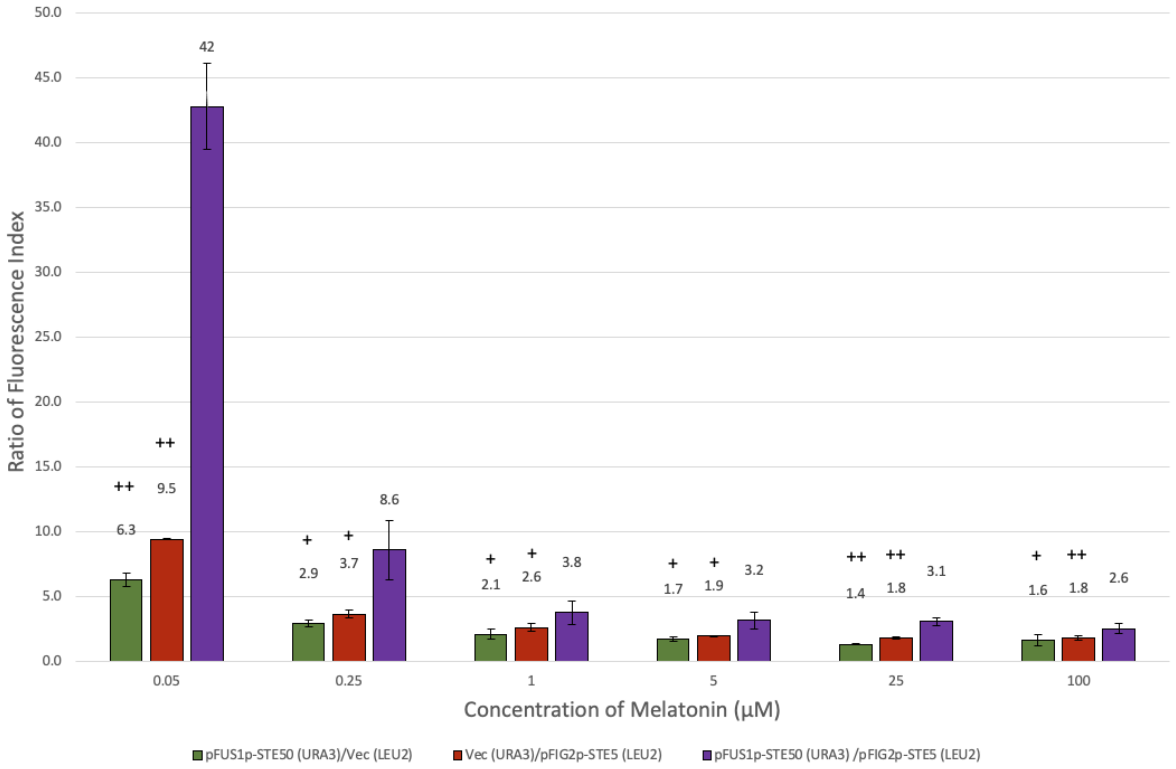

Figure 16. The relative effects of different feedback loops on the yeast melatonin biosensor at different concentrations of melatonin. The calculated ratio between *pFUS1p-STE50* (*URA3*)/Vec (*LEU2*) to Vec (*URA3*)/Vec (*LEU2*) is seen in Green, Vec (*URA3*)/*pFIG2p-STE5* (*LEU2*) to Vec (*URA3*)/Vec (*LEU2*) is seen in Red and *pFUS1p-STE50* (*URA3*)/*pFIG2p-STE5* (*LEU2*) to Vec (*URA3*)/Vec (*LEU2*) is seen in Purple. (+, P-values in respect to *pFUS1p-STE50*/*pFIG2p-STE5*; +, P < 0.05; ++, P < 0.01; +++ P <0.001)

CHAPTER 4: DISCUSSION

GPCR systems that function with the yeast pheromone pathway have been used as a tool in the discovery of novel drugs, such as Lorazepam, an anxiety disorder medication [99]. However, several complications, such as associating specific molecular targets to specific diseases in the early stages of the drug development process, have prevented new drugs from coming to market as GPCR agonists or antagonists. In this project we have taken a closer look at the GPCR-mediated signaling system of the yeast pheromone pathway to improve upon the pathway and its reporter output. We hypothesized that the addition of positive feedback loops on two different positive regulators would allow for an augmented signaling output and thus increased sensitivity of ligand sensing. The two different positive regulators of the pheromone pathway that we chose to study were *STE50* and *STE5*. We upregulated both genes individually and together and used transcriptional activation reporter assays to test if they increased the pheromone pathway signaling output. Two different pathway-activity-inducible reporters were used in this study; *HIS3* and GFP. The results show that with the *FIG1p-HIS3* reporter assay (in two to three days long-term scale) having more *STE50* does allow for better signaling as compared to the wildtype (**Compare B to A in Fig 13**). However, having more *STE5* alone or in combination with *STE50* as double feedback loops demonstrated a halo effect where no growth is observed, suggesting the elevated level of Ste5 may have caused Far1-independent cell cycle arrest, perhaps because it shares sequence similarity with Far1, and this makes it impossible to score for long-term cell growth (**C and D in Fig 13**). Interestingly, however, when assayed using the GFP reporter with the melatonin biosensor for 4-hours of treatment, the single positive feedback loops of either *STE50* or *STE5* alone did allow a significant increase in GFP output with P-value < 0.05 (**Green and red in Fig 15**), while having dual feedback loops showed an even higher output with P-value < 0.05 (**Purple in Fig 15**).

4.1 Plasmid Selection for *STE50* and *STE5*

As previously mentioned, various combinations of Ste50 and Ste5 constructs were built to test the positive feedback loop system using different inducible promoters that can be activated by the mating pathway (**Table A2**). Overall, only a select few were chosen to experiment with the positive feedback loop and to observe the effects that overproducing Ste50, Ste5 or Ste50 and Ste5 have on the mating pathway's reporter output. This includes the *pFUS1p-STE50* to over-produce Ste50 and *pFIG2p-STE5* to over-produce Ste5. Constructs that were built containing *GAL1p* were used in the early phase of the study as a positive control to show that elevated levels of the chosen positive regulators indeed lead to increased signaling output; however, the constant elevated level of the positive regulator cause highly elevated basal levels of pathway activity (Data not shown). The *GAL1p* driven construct was dropped in the later phase of the study. Also, we did not further the study with the *ste50* mutants on *FUS1p* or *FIG2p* as promotors, as their performance and output showed no significant difference from the wildtype Ste50 strain (Data not shown). *STE5* was originally designed with *FUS1p* or *FIG2p* as promoters but we later discontinued *pFUS1p-STE5* as it contained a higher basal level of activity which might cause cell cycle arrest at high concentration of α-factor or melatonin when doing a spotting assay or GFP assay (Data not shown).

4.2 Transcriptional Activation of *HIS3* Reporter for Reverse Halo Assay

Transcriptional activation of the *HIS3* gene was done to observe the long-term effects of overproducing Ste50 and Ste5 through controlled feedback loops. Initial experiments with the *HIS3* reporter were done using the *ste50* knockout strains YCW311, YST100 (YCW311 *sst1Δ*), YST200 (YCW311 *far1Δ*), YST300 (YCW311 *sst1Δ far1Δ).* These strains allowed us to test our *STE50* constructs and demonstrate that Ste50 is a positive regulator of the pathway and that

elevated levels of *STE50* increases the pheromone pathway output (**Fig 9**). They also recapitulated the importance of removing the negative regulators *bar1/sst1* (**Fig 7 and 9**) and *far1* (**Fig 8 and 9**) to prevent pheromone from getting cleaved or cell cycle arrest, respectively.

We then switched to the yWS677 derivative[98] and created different derivatives, YCW2432 (YCW2405 *FUS1p-HIS3*), YCW2433 (YCW2405 *FIG1p-HIS3*) and YCW2434 (YCW2405 *FIG2p-HIS3).* The parental strain and its derivatives contain only the essential components of the pheromone pathway making it easier to use it for testing our hypothesis on positive feedback loops. They all have chromosomal copies of both *STE50* and *STE5* such that the effect of additional copies of Ste50 and Ste5 in signaling can be assessed. In addition, these strains have better multi-plasmid marker selection compatibility.

Before testing our hypothesis with the positive feedback loops, we had to select one of the derivatives for the reverse halo assay. Therefore, we performed the spotting assay on all three derivatives and the parental strain in the absence or presence of 5.6 μM α-factor to first test for the lowest basal activity and then for transcriptional activation of the *HIS3* reporter (**Fig 10**). Each of the derivatives had a different basal level pathway activity. The inability of these strains to grow in medium with 3-AT concentrations higher than 1 mM demonstrates how well the pheromone inducible promoters are suppressed in these strains (**See B1, C1 and D1 in Fig 10**). The *HIS3* reporters in the strains were well repressed in the absence of pheromone and fully inducible to a wide range of activities. Going forward we used YCW2433 (YCW2405 *FIG1p-HIS3*) as the biosensor for *HIS3* reporter assays as it showed the lowest basal activity of the three strains and used pheromone-inducible promoters differently from the those used in the feedback-generating *pFUS1p-STE50* and *pFIG2p-STE5* constructs, avoiding potential competing effects for transcriptional activation factors and promoter binding. A spotting assay was redone with this

strain in the presence of my two-plasmid system to observe if having my constructs affected the strain's basal level (**Fig 11**). As no change was observed in the strain's performance, we moved to the reverse halo assay.

The reverse halo assay performed with both 5 mM and 10 mM 3-AT yielded similar results with Ste50, demonstrating higher levels of signaling as compared to the control (**A and B in Fig 13**), whereas Ste5 alone and in combination with Ste50 initially demonstrated a higher response followed by cell cycle arrest (**C and D in Fig 13**). Various reasons may be linked to the results seen in the Ste5 feedback loop as past studies have mentioned that overexpression of Ste5 suppresses the *far1* defect in pheromone induced cell cycle arrest[77]. Other studies have shown that Ste5 and Far1 are scaffold proteins with some degree of sequence and structure similarity in regions such as the RING and PH domains[75–77] (**Fig 6**). These domains are also found similar sequences throughout the entire fungal kingdom[75]. Due to the previous observations, there is reasonable evidence that those similar domains may be the reasons why mislocalization of the over-produced Ste5 can lead to Far1-independent cell cycle arrest. A noticeable difference between 5 mM and 10 mM 3-AT plates is that at 10 mM the yeast with control vectors is incapable of growing at 70 nM and 35 nM of α-factor (**See A in Fig 13**). This makes sense as 10 mM 3-AT is much more inhibitive towards the *HIS3* gene product, and thus would require higher level transcriptional activation of the *FIG1p-HIS3* of the strain to make enough His3p to allow growth at the toxic levels of 3-AT.

4.3 Transcriptional activation of GFP for a Melatonin Biosensor

Short-term effects of over-producing Ste50 and Ste5 through the controlled positive feedback loops demonstrated that having both Ste50 and Ste5 together generated higher average fluorescence index (**See purple in Fig 15**) with calculated P-values of < 0.05, as compared to either alone or to the vector control at every concentration of melatonin tested. While these results show that the controlled feedback loops are effective, they do not demonstrate how much more effective these constructs are compared to the control. Therefore, to compare each of the feedback loops to the vector only, the ratio of each average fluorescence index to the control's average fluorescence index at every concentration of melatonin (except those below 0.05 μM) was plotted (**Fig 16**). Concentrations below 0.05 μM were not included due to high basal levels of the Ste5 construct containing *FIG2* promoter as the ratio may not be a true representative comparison between the feedback loop versus the vector alone. Concentrations below 1 μM demonstrated a much higher ratio of fluorescence index than did those concentrations higher than 1 μM, with the dual feedback loop demonstrating a significantly more sensitive pathway, with P-values < 0.05, compared to either single feedback loop alone (**Compare green and red to purple in Fig 16**). This may be because the pathway with the feedback loop is much more sensitive at lower concentrations of melatonin as compared to higher concentrations of melatonin. This is greatly beneficial for biosensors as they would require lower levels of their ligand to be detectable. Overall, we observed that having an extra copy of Ste50 and/or Ste5 that is controlled by the positive feedback loop is better than the vector alone and that having both combined elicits an even greater effect with enhanced sensitivity at low ligand concentration range.

CHAPTER 5: CONCLUSIONS AND FUTURE DIRECTIONS

Improving the weak signaling output found in GPCR-mediated pathway signaling can enhance the sensitivity of a platform allowing for better detection of ligands to known receptors. We present a solution to enhance weak signaling through a controlled positive feedback loop that is activated by the signaling of the yeast pheromone pathway. We manipulated two positive regulators, *STE50* and *STE5* such that their expression is upregulated through an inducible promoter either individually or in combination. This was done to observe the effect of using two different yeast strains with different reporters to compare both long-term and short-term effects. The *HIS3* auxotrophic reporter was used for the long-term effect of over-producing *STE50* and *STE5* whereas the GFP reporter was used with a melatonin biosensor to observe the short-term effects. What was observed was that an increase in Ste50 through a positive feedback loop gave increased signaling output that could be measured through both long-term and short-term assays. As for Ste5, over-production through a positive feedback loop demonstrated increased signaling that can be measured in the short-term. However, measuring in the long-term is compromised by the Far1-independent cell cycle arrest that occurs due to elevated levels of Ste5. A combined positive feedback loop system of Ste50 and Ste5 in the short-term demonstrates a greater signal strength than either alone.

Although high levels of Ste5 causing Far1-indpendent cell cycle arrest complicated the long-term reporter assay, it provided experimental conditions to look for Ste5 mutants defective in causing Far1-indendent cell cycle arrest when overexpressed. Such mutants, if found, should provide an opportunity to examine the role of Ste5 in MAPK pathway activation separable from its role in Far1-indedpendent cell cycle arrest. This should further our mechanistic understanding of how this multifunctional prototype scaffold works. Future directions for this project include

closely examining select mutant types of *STE5* that separate its function in pathway activation from its role in Far1-independent cell cycle arrest when overproduced in the long-term assay. From the reverse halo assay, we were able to select a few potential mutants that could grow within the halo of cell growth inhibition in the presence of α-factor. Those cells were grown, and the plasmid constructs were isolated and put back into both YCW2433 and YCW2418 for assaying. One of the mutants showed promising results in the short-term assay while another showed promising results in the long-term assay. Sending those plasmids for sequencing to determine what those potential mutations might help in understanding the role that Ste5 plays and how it can be disconnected from its role in cell cycle arrest when over-produced, as well as providing lower basal levels in GFP reporter cells compared to its wild-type counterpart. In addition, possibly testing known weak heterologous GPCRs with the improved systems from this study will determine if enhancing the output is generally applicable.

REFERENCES:

(1) Wacker, D.; Stevens, R. C.; Roth, B. L. How Ligands Illuminate GPCR Molecular Pharmacology. *Cell* **2017**, *170* (3), 414–427. https://doi.org/10.1016/j.cell.2017.07.009.

(2) Mirzadegan, T.; Benkö, G.; Filipek, S.; Palczewski, K. Sequence Analyses of G-Protein-Coupled Receptors: Similarities to Rhodopsin. *Biochemistry* **2003**, *42* (14), 4310–4310. https://doi.org/10.1021/bi033002f.

(3) Hamm, H. E.; Gilchrist, A. Heterotrimeric G Proteins. *Curr Opin Cell Biol* **1996**, *8* (2), 189–196. https://doi.org/10.1016/S0955-0674(96)80065-2.

(4) Mombaerts, P. Genes and Ligands for Odorant, Vomeronasal and Taste Receptors. *Nat Rev Neurosci* **2004**, *5* (4), 263–278. https://doi.org/10.1038/nrn1365.

(5) Lefkowitz, R. J. The Superfamily of Heptahelical Receptors. *Nat Cell Biol* **2000**, *2* (7), E133–E136. https://doi.org/10.1038/35017152.

(6) Strader, C. D.; Fong, T. M.; Tota, M. R.; Underwood, D.; Dixon, R. A. F. Structure and Function of G Protein-Coupled Receptors. *Annu Rev Biochem* **1994**, *63* (1), 101–132. https://doi.org/10.1146/annurev.bi.63.070194.000533.

(7) Gilman, A. G. G Proteins: Transducers of Receptor-Generated Signals. *Annu Rev Biochem* **1987**, *56* (1), 615–649. https://doi.org/10.1146/annurev.bi.56.070187.003151.

(8) Sriram, K.; Insel, P. A. G Protein-Coupled Receptors as Targets for Approved Drugs: How Many Targets and How Many Drugs? *Mol Pharmacol* **2018**, *93* (4), 251–258. https://doi.org/10.1124/mol.117.111062.

(9) Vassilatis, D. K.; Hohmann, J. G.; Zeng, H.; Li, F.; Ranchalis, J. E.; Mortrud, M. T.; Brown, A.; Rodriguez, S. S.; Weller, J. R.; Wright, A. C.; Bergmann, J. E.; Gaitanaris, G. A. The G Protein-Coupled Receptor Repertoires of Human and Mouse. *Proceedings of the National Academy of Sciences* **2003**, *100* (8), 4903–4908. https://doi.org/10.1073/pnas.0230374100.

(10) Salon, J. A.; Lodowski, D. T.; Palczewski, K. The Significance of G Protein-Coupled Receptor Crystallography for Drug Discovery. *Pharmacol Rev* **2011**, *63* (4), 901–937. https://doi.org/10.1124/pr.110.003350.

(11) Flower, D. R. Modelling G-Protein-Coupled Receptors for Drug Design. *Biochimica et Biophysica Acta (BBA) - Reviews on Biomembranes* **1999**, *1422* (3), 207–234. https://doi.org/10.1016/S0304-4157(99)00006-4.

(12) Robas, N. Maximizing Serendipity: Strategies for Identifying Ligands for Orphan G-Protein-Coupled Receptors. *Curr Opin Pharmacol* **2003**, *3* (2), 121–126. https://doi.org/10.1016/S1471-4892(03)00010-9.

(13) Overington, J. P.; Al-Lazikani, B.; Hopkins, A. L. How Many Drug Targets Are There? *Nat Rev Drug Discov* **2006**, *5* (12), 993–996. https://doi.org/10.1038/nrd2199.

(14) Pausch, M. H. G-Protein-Coupled Receptors in *Saccharomyces cerevisiae*: High-Throughput Screening Assays for Drug Discovery. *Trends Biotechnol* **1997**, *15* (12), 487–494. https://doi.org/10.1016/S0167-7799(97)01119-0.

(15) Dohlman, H. G.; Thorner, J.; Caron, M. G.; Lefkowitz, R. J. Model Systems for the Study of Seven-Transmembrane-Segment Receptors. *Annu Rev Biochem* **1991**, *60* (1), 653–688. https://doi.org/10.1146/annurev.bi.60.070191.003253.

(16) Brown, A. J.; Dyos, S. L.; Whiteway, M. S.; White, J. H. M.; Watson, M.-A. E. A.; Marzioch, M.; Clare, J. J.; Cousens, D. J.; Paddon, C.; Plumpton, C.; Romanos, M. A.; Dowell, S. J. Functional Coupling of Mammalian Receptors to the Yeast Mating Pathway Using Novel Yeast/Mammalian G Protein α-Subunit Chimeras. *Yeast* **2000**, *16* (1), 11–22. https://doi.org/10.1002/(SICI)1097-0061(20000115)16:1<11::AID-YEA502>3.0.CO;2-K.

(17) Ault, A. D.; Broach, J. R. Creation of GPCR-Based Chemical Sensors by Directed Evolution in Yeast. *Protein Engineering, Design and Selection* **2006**, *19* (1), 1–8. https://doi.org/10.1093/protein/gzi069.

(18) Armbruster, B. N.; Li, X.; Pausch, M. H.; Herlitze, S.; Roth, B. L. Evolving the Lock to Fit the Key to Create a Family of G Protein-Coupled Receptors Potently Activated by an Inert Ligand. *Proceedings of the National Academy of Sciences* **2007**, *104* (12), 5163–5168. https://doi.org/10.1073/pnas.0700293104.

(19) Conklin, B. R.; Hsiao, E. C.; Claeysen, S.; Dumuis, A.; Srinivasan, S.; Forsayeth, J. R.; Guettier, J.-M.; Chang, W. C.; Pei, Y.; McCarthy, K. D.; Nissenson, R. A.; Wess, J.; Bockaert, J.; Roth, B. L. Engineering GPCR Signaling Pathways with RASSLs. *Nat Methods* **2008**, *5* (8), 673–678. https://doi.org/10.1038/nmeth.1232.

(20) Dong, S.; Rogan, S. C.; Roth, B. L. Directed Molecular Evolution of DREADDs: A Generic Approach to Creating Next-Generation RASSLs. *Nat Protoc* **2010**, *5* (3), 561–573. https://doi.org/10.1038/nprot.2009.239.

(21) Ishii, J.; Matsumura, S.; Kimura, S.; Tatematsu, K.; Kuroda, S.; Fukuda, H.; Kondo, A. Quantitative and Dynamic Analyses of G Protein-Coupled Receptor Signaling in Yeast Using Fus1, Enhanced Green Fluorescence Protein (*EGFP*), and His3 Fusion Protein. *Biotechnol Prog* **2006**, *22* (4), 954–960. https://doi.org/10.1021/bp0601387.

(22) Beukers, M. W.; Ijzerman, A. P. Techniques: How to Boost GPCR Mutagenesis Studies Using Yeast. *Trends Pharmacol Sci* **2005**, *26* (10), 533–539. https://doi.org/10.1016/j.tips.2005.08.005.

(23) *BioRender*. https://app.biorender.com/.

(24) Rowe, J. B.; Taghon, G. J.; Kapolka, N. J.; Morgan, W. M.; Isom, D. G. CRISPR-Addressable Yeast Strains with Applications in Human G Protein–Coupled Receptor Profiling and Synthetic Biology. *Journal of Biological Chemistry* **2020**, *295* (24), 8262–8271. https://doi.org/10.1074/jbc.RA120.013066.

(25) Kraakman, L.; Lemaire, K.; Ma, P.; Teunissen, A. W. R. H.; Donaton, M. C. V.; van Dijck, P.; Winderickx, J.; de Winde, J. H.; Thevelein, J. M. A *Saccharomyces cerevisiae* G-Protein Coupled Receptor, Gpr1, is Specifically Required for Glucose Activation of the CAMP Pathway during the Transition to Growth on Glucose. *Mol Microbiol* **1999**, *32* (5), 1002–1012. https://doi.org/10.1046/j.1365-2958.1999.01413.x.

(26) Yun, C.-W.; Tamaki, H.; Nakayama, R.; Yamamoto, K.; Kumagai, H. G-Protein Coupled Receptor from Yeast *Saccharomyces cerevisiae*. *Biochem Biophys Res Commun* **1997**, *240* (2), 287–292. https://doi.org/10.1006/bbrc.1997.7649.

(27) Mackay, V.; Manney, T. R. Mutations Affecting Sexual Conjugation and Related Processes in *Saccharomyces cerevisiae*. II. Genetic Analysis of Nonmating Mutants. *Genetics* **1974**, *76* (2), 273–288. https://doi.org/10.1093/genetics/76.2.273.

(28) Nakafuku, M.; Obara, T.; Kaibuchi, K.; Miyajima, I.; Miyajima, A.; Itoh, H.; Nakamura, S.; Arai, K.; Matsumoto, K.; Kaziro, Y. Isolation of a Second Yeast *Saccharomyces cerevisiae* Gene (*GPA2*) Coding for Guanine Nucleotide-Binding Regulatory Protein: Studies on Its Structure and Possible Functions. *Proceedings of the National Academy of Sciences* **1988**, *85* (5), 1374–1378. https://doi.org/10.1073/pnas.85.5.1374.

(29) Lorenz, M. C.; Pan, X.; Harashima, T.; Cardenas, M. E.; Xue, Y.; Hirsch, J. P.; Heitman, J. The G Protein-Coupled Receptor Gpr1 is a Nutrient Sensor That Regulates Pseudohyphal Differentiation in *Saccharomyces cerevisiae*. *Genetics* **2000**, *154* (2), 609–622. https://doi.org/10.1093/genetics/154.2.609.

(30) Harashima, T.; Heitman, J. The Gα Protein Gpa2 Controls Yeast Differentiation by Interacting with Kelch Repeat Proteins That Mimic Gβ Subunits. *Mol Cell* **2002**, *10* (1), 163–173. https://doi.org/10.1016/S1097-2765(02)00569-5.

(31) Harashima, T.; Heitman, J. 6 Nutrient Control of Dimorphic Growth in *Saccharomyces cerevisiae*; 2004; pp 131–169. https://doi.org/10.1007/978-3-540-39898-1_7.

(32) Lambright, D. G.; Sondek, J.; Bohm, A.; Skiba, N. P.; Hamm, H. E.; Sigler, P. B. The 2.0 Å Crystal Structure of a Heterotrimeric G Protein. *Nature* **1996**, *379* (6563), 311–319. https://doi.org/10.1038/379311a0.

(33) Adams, J.; Kelso, R.; Cooley, L. The Kelch Repeat Superfamily of Proteins: Propellers of Cell Function. *Trends Cell Biol* **2000**, *10* (1), 17–24. https://doi.org/10.1016/S0962-8924(99)01673-6.

(34) Sondek, J.; Bohm, A.; Lambright, D. G.; Hamm, H. E.; Sigler, P. B. Crystal Structure of a G_A Protein βγdimer at 2.1 Å Resolution. *Nature* **1996**, *379* (6563), 369–374. https://doi.org/10.1038/379369a0.

(35) Wall, M. A.; Coleman, D. E.; Lee, E.; Iñiguez-Lluhi, J. A.; Posner, B. A.; Gilman, A. G.; Sprang, S. R. The Structure of the G Protein Heterotrimer Giα1β1γ2. *Cell* **1995**, *83* (6), 1047–1058. https://doi.org/10.1016/0092-8674(95)90220-1.

(36) Dietzel, C.; Kurjan, J. The Yeast *SCG1* Gene: A Gα-like Protein Implicated in the a- and α-Factor Response Pathway. *Cell* **1987**, *50* (7), 1001–1010. https://doi.org/10.1016/0092-8674(87)90166-8.

(37) Whiteway, M.; Hougan, L.; Dignard, D.; Thomas, D. Y.; Bell, L.; Saari, G. C.; Grant, F. J.; O'Hara, P.; MacKay, V. L. The *STE4* and *STE18* Genes of Yeast Encode Potential β and γ Subunits of the Mating Factor Receptor-Coupled G Protein. *Cell* **1989**, *56* (3), 467–477. https://doi.org/10.1016/0092-8674(89)90249-3.

(38) Liao, H.; Thorner, J. Yeast Mating Pheromone Alpha Factor Inhibits Adenylate Cyclase. *Proceedings of the National Academy of Sciences* **1980**, *77* (4), 1898–1902. https://doi.org/10.1073/pnas.77.4.1898.

(39) Chaleff, D. T.; Tatchell, K. Molecular Cloning and Characterization of the *STE7* and *STE11* Genes of *Saccharomyces cerevisiae*. *Mol Cell Biol* **1985**, *5* (8), 1878–1886. https://doi.org/10.1128/mcb.5.8.1878-1886.1985.

(40) Wu, C.; Leberer, E.; Thomas, D. Y.; Whiteway, M. Functional Characterization of the Interaction of Ste50p with Ste11p MAPKKK in *Saccharomyces cerevisiae*. *Mol Biol Cell* **1999**, *10* (7), 2425–2440. https://doi.org/10.1091/mbc.10.7.2425.

(41) Elion, E. A.; Grisafi, P. L.; Fink, G. R. *FUS3* Encodes a Cdc2+/CDC28-Related Kinase Required for the Transition from Mitosis into Conjugation. *Cell* **1990**, *60* (4), 649–664. https://doi.org/10.1016/0092-8674(90)90668-5.

(42) Leberer, E.; Dignard, D.; Harcus, D.; Thomas, D. Y.; Whiteway, M. The Protein Kinase Homologue Ste20p is Required to Link the Yeast Pheromone Response G-Protein Beta Gamma Subunits to Downstream Signalling Components. *EMBO J* **1992**, *11* (13), 4815–4824. https://doi.org/10.1002/j.1460-2075.1992.tb05587.x.

(43) Elion, E. A. Ste5: A Meeting Place for MAP Kinases and their Associates. *Trends Cell Biol* **1995**, *5* (8), 322–327. https://doi.org/10.1016/S0962-8924(00)89055-8.

(44) Errede, B.; Gartner, A.; Zhou, Z.; Nasmyth, K.; Ammerer, G. MAP Kinase-Related *FUS3* from *S. cerevisiae* is Activated by *STE7 in vitro*. *Nature* **1993**, *362* (6417), 261–264. https://doi.org/10.1038/362261a0.

(45) Cook, J. G.; Bardwell, L.; Kron, S. J.; Thorner, J. Two Novel Targets of the MAP Kinase Kss1 Are Negative Regulators of Invasive Growth in the Yeast *Saccharomyces cerevisiae*. *Genes Dev* **1996**, *10* (22), 2831–2848. https://doi.org/10.1101/gad.10.22.2831.

(46) Tedford, K.; Kim, S.; Sa, D.; Stevens, K.; Tyers, M. Regulation of the Mating Pheromone and Invasive Growth Responses in Yeast by Two MAP Kinase Substrates. *Current Biology* **1997**, *7* (4), 228–238. https://doi.org/10.1016/S0960-9822(06)00118-7.

(47) Errede, B.; Ammerer, G. *STE12*, a Protein Involved in Cell-Type-Specific Transcription and Signal Transduction in Yeast, is Part of Protein-DNA Complexes. *Genes Dev* **1989**, *3* (9), 1349–1361. https://doi.org/10.1101/gad.3.9.1349.

(48) Chang, F.; Herskowitz, I. Identification of a Gene Necessary for Cell Cycle Arrest by a Negative Growth Factor of Yeast: *FAR1* is an Inhibitor of a G1 Cyclin, *CLN2*. *Cell* **1990**, *63* (5), 999–1011. https://doi.org/10.1016/0092-8674(90)90503-7.

(49) Gartner, A.; Nasmyth, K.; Ammerer, G. Signal Transduction in *Saccharomyces cerevisiae* Requires Tyrosine and Threonine Phosphorylation of *FUS3* and *KSS1*. *Genes Dev* **1992**, *6* (7), 1280–1292. https://doi.org/10.1101/gad.6.7.1280.

(50) Kohno, H.; Tanaka, K.; Mino, A.; Umikawa, M.; Imamura, H.; Fujiwara, T.; Fujita, Y.; Hotta, K.; Qadota, H.; Watanabe, T.; Ohya, Y.; Takai, Y. Bni1p Implicated in Cytoskeletal Control is a Putative Target of Rho1p Small GTP Binding Protein in *Saccharomyces cerevisiae*. *EMBO J* **1996**, *15* (22), 6060–6068. https://doi.org/10.1002/j.1460-2075.1996.tb00994.x.

(51) Matheos, D.; Metodiev, M.; Muller, E.; Stone, D.; Rose, M. D. Pheromone-Induced Polarization is Dependent on the Fus3p MAPK Acting through the Formin Bni1p. *Journal of Cell Biology* **2004**, *165* (1), 99–109. https://doi.org/10.1083/jcb.200309089.

(52) Chan, R. K.; Otte, C. A. Isolation and Genetic Analysis of *Saccharomyces cerevisiae* Mutants Supersensitive to G1 Arrest by a Factor and Alpha Factor Pheromones. *Mol Cell Biol* **1982**, *2* (1), 11–20. https://doi.org/10.1128/mcb.2.1.11-20.1982.

(53) Dietzel, C.; Kurjan, J. Pheromonal Regulation and Sequence of the *Saccharomyces cerevisiae SST2* Gene: A Model for Desensitization to Pheromone. *Mol Cell Biol* **1987**, *7* (12), 4169–4177. https://doi.org/10.1128/mcb.7.12.4169-4177.1987.

(54) Sprague, G. F.; Herskowitz, I. Control of Yeast Cell Type by the Mating Type Locus. *J Mol Biol* **1981**, *153* (2), 305–321. https://doi.org/10.1016/0022-2836(81)90280-1.

(55) Chan, R. K.; Otte, C. A. Physiological Characterization of *Saccharomyces cerevisiae* Mutants Supersensitive to G1 Arrest by a Factor and Alpha Factor Pheromones. *Mol Cell Biol* **1982**, *2* (1), 21–29. https://doi.org/10.1128/mcb.2.1.21-29.1982.

(56) Kofahl, B.; Klipp, E. Modelling the Dynamics of the Yeast Pheromone Pathway. *Yeast* **2004**, *21* (10), 831–850. https://doi.org/10.1002/yea.1122.

(57) Chasse, S. A.; Flanary, P.; Parnell, S. C.; Hao, N.; Cha, J. Y.; Siderovski, D. P.; Dohlman, H. G. Genome-Scale Analysis Reveals Sst2 as the Principal Regulator of Mating Pheromone Signaling in the Yeast *Saccharomyces cerevisiae*. *Eukaryot Cell* **2006**, *5* (2), 330–346. https://doi.org/10.1128/EC.5.2.330-346.2006.

(58) Hadwiger, J. A.; Wittenberg, C.; Richardson, H. E.; de Barros Lopes, M.; Reed, S. I. A Family of Cyclin Homologs That Control the G1 Phase in Yeast. *Proceedings of the National Academy of Sciences* **1989**, *86* (16), 6255–6259. https://doi.org/10.1073/pnas.86.16.6255.

(59) Chang, F.; Herskowitz, I. Phosphorylation of *FAR1* in Response to Alpha-Factor: A Possible Requirement for Cell-Cycle Arrest. *Mol Biol Cell* **1992**, *3* (4), 445–450. https://doi.org/10.1091/mbc.3.4.445.

(60) Jones, S. K.; Clarke, S. C.; Craik, C. S.; Bennett, R. J. Evolutionary Selection on Barrier Activity: Bar1 is an Aspartyl Protease with Novel Substrate Specificity. *mBio* **2015**, *6* (6). https://doi.org/10.1128/mBio.01604-15.

(61) Struhl, K.; Davis, R. W. Production of a Functional Eukaryotic Enzyme in *Escherichia coli*: Cloning and Expression of the Yeast Structural Gene for Imidazole-Glycerolphosphate Dehydratase (His3). *Proceedings of the National Academy of Sciences* **1977**, *74* (12), 5255–5259. https://doi.org/10.1073/pnas.74.12.5255.

(62) Horecka, J.; Sprague, G. F. Use of Imidazoleglycerolphosphate Dehydratase (His3) as a Biological Reporter in Yeast; 2000; pp 107–119. https://doi.org/10.1016/S0076-6879(00)26049-7.

(63) Cormack, B. P.; Bertram, G.; Egerton, M.; Gow, N. A. R.; Falkow, S.; Brown, A. J. P. Yeast-Enhanced Green Fluorescent Protein (*YEGFP*): A Reporter of Gene Expression in Candida Albicans. *Microbiology (N Y)* **1997**, *143* (2), 303–311. https://doi.org/10.1099/00221287-143-2-303.

(64) Rupp, S. LacZ Assays in Yeast; 2002; pp 112–131. https://doi.org/10.1016/S0076-6879(02)50959-9.

(65) Shaw, W. M.; Yamauchi, H.; Mead, J.; Gowers, G.-O. F.; Bell, D. J.; Öling, D.; Larsson, N.; Wigglesworth, M.; Ladds, G.; Ellis, T. Engineering a Model Cell for Rational Tuning of GPCR Signaling. *Cell* **2019**, *177* (3), 782-796.e27. https://doi.org/10.1016/j.cell.2019.02.023.

(66) Trueheart, J.; Boeke, J. D.; Fink, G. R. Two Genes Required for Cell Fusion during Yeast Conjugation: Evidence for a Pheromone-Induced Surface Protein. *Mol Cell Biol* **1987**, *7* (7), 2316–2328. https://doi.org/10.1128/mcb.7.7.2316-2328.1987.

(67) Erdman, S.; Lin, L.; Malczynski, M.; Snyder, M. Pheromone-Regulated Genes Required for Yeast Mating Differentiation. *Journal of Cell Biology* **1998**, *140* (3), 461–483. https://doi.org/10.1083/jcb.140.3.461.

(68) Sharmeen, N.; Sulea, T.; Whiteway, M.; Wu, C. The Adaptor Protein Ste50 Directly Modulates Yeast MAPK Signaling Specificity through Differential Connections of Its RA Domain. *Mol Biol Cell* **2019**, *30* (6), 794–807. https://doi.org/10.1091/mbc.E18-11-0708.

(69) Wu, C.; Jansen, G.; Zhang, J.; Thomas, D. Y.; Whiteway, M. Adaptor Protein Ste50p Links the Ste11p MEKK to the HOG Pathway through Plasma Membrane Association. *Genes Dev* **2006**, *20* (6), 734–746. https://doi.org/10.1101/gad.1375706.

(70) Elion, E. A. The Ste5p Scaffold. *J Cell Sci* **2001**, *114* (22), 3967–3978. https://doi.org/10.1242/jcs.114.22.3967.

(71) Garrenton, L. S.; Braunwarth, A.; Irniger, S.; Hurt, E.; Künzler, M.; Thorner, J. Nucleus-Specific and Cell Cycle-Regulated Degradation of Mitogen-Activated Protein Kinase Scaffold Protein Ste5 Contributes to the Control of Signaling Competence. *Mol Cell Biol* **2009**, *29* (2), 582–601. https://doi.org/10.1128/MCB.01019-08.

(72) Xu, G.; Jansen, G.; Thomas, D. Y.; Hollenberg, C. P.; Rad, M. R. Ste50p Sustains Mating Pheromone-Induced Signal Transduction in the Yeast *Saccharomyces cerevisiae*. *Mol Microbiol* **1996**, *20* (4), 773–783. https://doi.org/10.1111/j.1365-2958.1996.tb02516.x.

(73) Edwards, M. C.; Liegeois, N.; Horecka, J.; DePinho, R. A.; Sprague, G. F.; Tyers, M.; Elledge, S. J. Human *CPR* (Cell Cycle Progression Restoration) Genes Impart a Far– Phenotype on Yeast Cells. *Genetics* **1997**, *147* (3), 1063–1076. https://doi.org/10.1093/genetics/147.3.1063.

(74) Zalatan, J. G.; Coyle, S. M.; Rajan, S.; Sidhu, S. S.; Lim, W. A. Conformational Control of the Ste5 Scaffold Protein Insulates Against MAP Kinase Misactivation. *Science (1979)* **2012**, *337* (6099), 1218–1222. https://doi.org/10.1126/science.1220683.

(75) Côte, P.; Sulea, T.; Dignard, D.; Wu, C.; Whiteway, M. Evolutionary Reshaping of Fungal Mating Pathway Scaffold Proteins. *mBio* **2011**, *2* (1). https://doi.org/10.1128/mBio.00230-10.

(76) Inouye, C.; Dhillon, N.; Thorner, J. Ste5 RING-H2 Domain: Role in Ste4-Promoted Oligomerization for Yeast Pheromone Signaling. *Science (1979)* **1997**, *278* (5335), 103–106. https://doi.org/10.1126/science.278.5335.103.

(77) Leberer, E.; Dignard, D.; Harcus, D.; Hougan, L.; Whiteway, M.; Thomas, D. Y. Cloning of *Saccharomyces cerevisiae STE5* as a Suppressor of a Ste20 Protein Kinase Mutant: Structural and Functional Similarity of Ste5 to Farl. *Mol Gen Genet* **1993**, *241–241* (3–4), 241–254. https://doi.org/10.1007/BF00284675.

(78) Kranz, J. E.; Satterberg, B.; Elion, E. A. The MAP Kinase Fus3 Associates with and Phosphorylates the Upstream Signaling Component Ste5. *Genes Dev* **1994**, *8* (3), 313–327. https://doi.org/10.1101/gad.8.3.313.

(79) Good, M.; Tang, G.; Singleton, J.; Reményi, A.; Lim, W. A. The Ste5 Scaffold Directs Mating Signaling by Catalytically Unlocking the Fus3 MAP Kinase for Activation. *Cell* **2009**, *136* (6), 1085–1097. https://doi.org/10.1016/j.cell.2009.01.049.

(80) Oldenburg, K. Recombination-Mediated PCR-Directed Plasmid Construction *in Vivo* in Yeast. *Nucleic Acids Res* **1997**, *25* (2), 451–452. https://doi.org/10.1093/nar/25.2.451.

(81) Mullis, K.; Faloona, F.; Scharf, S.; Saiki, R.; Horn, G.; Erlich, H. Specific Enzymatic Amplification of DNA In Vitro: The Polymerase Chain Reaction. *Cold Spring Harb Symp Quant Biol* **1986**, *51* (0), 263–273. https://doi.org/10.1101/SQB.1986.051.01.032.

(82) Baker Brachmann, C.; Davies, A.; Cost, G. J.; Caputo, E.; Li, J.; Hieter, P.; Boeke, J. D. Designer Deletion Strains Derived from *Saccharomyces cerevisiae* S288C: A Useful Set of Strains and Plasmids for PCR-Mediated Gene Disruption and Other Applications. *Yeast* **1998**, *14* (2), 115–132. https://doi.org/10.1002/(SICI)1097-0061(19980130)14:2<115::AID-YEA204>3.0.CO;2-2.

(83) Chen, D.-C.; Yang, B.-C.; Kuo, T.-T. One-Step Transformation of Yeast in Stationary Phase. *Curr Genet* **1992**, *21* (1), 83–84. https://doi.org/10.1007/BF00318659.

(84) Bryksin, A. v.; Matsumura, I. Overlap Extension PCR Cloning: A Simple and Reliable Way to Create Recombinant Plasmids. *Biotechniques* **2010**, *48* (6), 463–465. https://doi.org/10.2144/000113418.

(85) Ishino, Y.; Shinagawa, H.; Makino, K.; Amemura, M.; Nakata, A. Nucleotide Sequence of the *Iap* Gene, Responsible for Alkaline Phosphatase Isozyme Conversion in *Escherichia coli*, and Identification of the Gene Product. *J Bacteriol* **1987**, *169* (12), 5429–5433. https://doi.org/10.1128/jb.169.12.5429-5433.1987.

(86) DiCarlo, J. E.; Norville, J. E.; Mali, P.; Rios, X.; Aach, J.; Church, G. M. Genome Engineering in *Saccharomyces cerevisiae* Using CRISPR-Cas Systems. *Nucleic Acids Res* **2013**, *41* (7), 4336–4343. https://doi.org/10.1093/nar/gkt135.

(87) Neldeborg, S.; Lin, L.; Stougaard, M.; Luo, Y. Rapid and Efficient Gene Deletion by CRISPR/Cas9; 2019; pp 233–247. https://doi.org/10.1007/978-1-4939-9170-9_14.

(88) Laughery, M. F.; Hunter, T.; Brown, A.; Hoopes, J.; Ostbye, T.; Shumaker, T.; Wyrick, J. J. New Vectors for Simple and Streamlined CRISPR-Cas9 Genome Editing in *Saccharomyces cerevisiae*. *Yeast* **2015**, *32* (12), 711–720. https://doi.org/10.1002/yea.3098.

(89) Miyaoka, Y.; Berman, J. R.; Cooper, S. B.; Mayerl, S. J.; Chan, A. H.; Zhang, B.; Karlin-Neumann, G. A.; Conklin, B. R. Systematic Quantification of HDR and NHEJ Reveals Effects of Locus, Nuclease, and Cell Type on Genome-Editing. *Sci Rep* **2016**, *6* (1), 23549. https://doi.org/10.1038/srep23549.

(90) *Addgene: pML104-KanMx4*. https://www.addgene.org/83476/?gclid=Cj0KCQjwgO2XBhCaARIsANrW2X0gGhQhMHziV16NddGlZBJFv1TCevVbJyi5jw2_oEisFi6ETJX0fiMaArWhEALw_wcB (Accessed 2022-08-22).

(91) *Addgene: pML107*. https://www.addgene.org/67639/?gclid=Cj0KCQjwgO2XBhCaARIsANrW2X028B5KTonOph9nfkpHjc8I0KhXR66QeWAkudhmJsviTpICjqx_8LQaAqPoEALw_wcB. (Accessed 2022-08-22).

(92) Sprague, G. F. Assay of Yeast Mating Reaction. In *Methods in Enzymology*; 1991; Vol. 194, pp 77–93. https://doi.org/10.1016/0076-6879(91)94008-Z.

(93) Price, L. A.; Kajkowski, E. M.; Hadcock, J. R.; Ozenberger, B. A.; Pausch, M. H. Functional Coupling of a Mammalian Somatostatin Receptor to the Yeast Pheromone Response Pathway. *Mol Cell Biol* **1995**, *15* (11), 6188–6195. https://doi.org/10.1128/MCB.15.11.6188.

(94) Koh, Y. Y.; Wickens, M. Identifying Proteins That Bind a Known RNA Sequence Using the Yeast Three-Hybrid System; 2014; pp 195–214. https://doi.org/10.1016/B978-0-12-420120-0.00011-6.

(95) Prasher, D. C.; Eckenrode, V. K.; Ward, W. W.; Prendergast, F. G.; Cormier, M. J. Primary Structure of the Aequorea Victoria Green-Fluorescent Protein. *Gene* **1992**, *111* (2), 229–233. https://doi.org/10.1016/0378-1119(92)90691-H.

(96) *Excitation and Emission of Green Fluorescent Proteins*. https://www.biotek.com/resources/technical-notes/excitation-and-emission-of-green-fluorescent-proteins/ (accessed 2022-08-22).

(97) McKinnon, K. M. Flow Cytometry: An Overview. *Curr Protoc Immunol* **2018**, *120* (1). https://doi.org/10.1002/cpim.40.

(98) Bean, B. D. M.; Mulvihill, C. J.; Garge, R. K.; Boutz, D. R.; Rousseau, O.; Floyd, B. M.; Cheney, W.; Gardner, E. C.; Ellington, A. D.; Marcotte, E. M.; Gollihar, J. D.; Whiteway, M.; Martin, V. J. J. Functional Expression of Opioid Receptors and Other Human GPCRs in Yeast Engineered to Produce Human Sterols. *Nat Commun* **2022**, *13* (1), 2882. https://doi.org/10.1038/s41467-022-30570-7.

(99) Huang, X.-P.; Karpiak, J.; Kroeze, W. K.; Zhu, H.; Chen, X.; Moy, S. S.; Saddoris, K. A.; Nikolova, V. D.; Farrell, M. S.; Wang, S.; Mangano, T. J.; Deshpande, D. A.; Jiang, A.; Penn, R. B.; Jin, J.; Koller, B. H.; Kenakin, T.; Shoichet, B. K.; Roth, B. L. Allosteric Ligands for the Pharmacologically Dark Receptors GPR68 and GPR65. *Nature* **2015**, *527* (7579), 477–483. https://doi.org/10.1038/nature15699.

(100) Weaver-Feldhaus, J. M.; Lou, J.; Coleman, J. R.; Siegel, R. W.; Marks, J. D.; Feldhaus, M. J. Yeast Mating for Combinatorial Fab Library Generation and Surface Display. *FEBS Lett* **2004**, *564* (1–2), 24–34. https://doi.org/10.1016/S0014-5793(04)00309-6.

APPENDIX

LIST OF TABLES

A SUMMARY OF YEAST STRAINS, PLASMIDS OLIGONUCLEOTIDES AND PCR REACTION CONDITIONS

Table A1. Yeast Strains Used in This Study

Strain	Genotype	Source
YCW311	*ste50Δ::TRP1 sst2::ura3 his3 leu2 ura3 trp1 FUS1-HIS3*	Lab strain
YST100	*ste50Δ::TRP1 sst2::ura3 sst1Δ his3 leu2 ura3 trp1 FUS1-HIS3*	This study
YST200	*ste50Δ::TRP1 sst2::ura3 far1Δ his3 leu2 ura3 trp1 FUS1-HIS3*	This study
YST300	*ste50Δ::TRP1 sst2::ura3 sst1Δ far1Δ his3 leu2 ura3 trp1 FUS1-HIS3*	This study
YCW2418	WCY67, (melatonin biosensor) BY4741 *fig1Δ::ENVY(gfp) sst2Δ ste2Δ GPA1(468-472Δ)-GNAI3(350-354)[EF]::PGK1p-MTNR1A-TDH1*	Reference 98
YCW1620	*W303-1A, ste5Δ::hisG FUS1-HIS3, his3 leu2 trp1 ura3*	Lab strain
YCW2405	YWS677 (BY4741 *sst2Δ far1Δ bar1Δ ste2Δ ste12Δ gpa1Δ ste3Δ mf(alpha)1Δ mf(alpha)2Δ mfa1Δ mfa2Δ gpr1Δ gpa2Δ)* derivative: *STE2, GPA1 STE12*	Reference 65
YCW2432	YCW2405 *FUS1p-HIS3*	This study
YCW2433	YCW2405 *FIG1p-HIS3*	This study
YCW2434	YCW2405 *FIG2p-HIS3*	This study
YCW57	*MATα his1*	Lab strain
YCW2052	*MAT**a** AGA1::GAL1AGA1::ura3::KanM4 ura3 trp1 leu2 his3 pep4::HIS3 can1*	Reference 100
YCW1886	*MAT**a** ste50Δ::Kan^R ssk1Δ::Nat^R sst1::hisG FUS1-LacZ::LEU2 his3 leu2 ura3 trp1 ade2*	Reference 68
YCW321	*MAT**a** sst1 sst2 kex2*	Lab strain
BY4741	*MATa his3Δ1 leu2Δ0 met15Δ0 ura3Δ0*	Lab strain

Table A2. Plasmids Built and Used in This Study

Summary of all constructs			
Name	**Promoter**	**Insert**	**Marker**
p416_*GAL1*	*GAL1p*		*URA3/AmpR*
p415_*GAL1*	*GAL1p*		*LEU2/AmpR*
pCW791	*STE50p*	*STE50(WT)*	*URA3/AmpR*
pCW791CC6E		*STE50(6E)*	*URA3/AmpR*
pCW791CC6G		*STE50(6G)*	*URA3/AmpR*
pGAL1p_STE50	*GAL1p*	*STE50(WT)*	*URA3/AmpR*
pGAL1p_STE50(6E)		*STE50(6E)*	*URA3/AmpR*
pGAL1p_STE50(6G)		*STE50(6G)*	*URA3/AmpR*
pFUS1p_STE50	*FUS1p*	*STE50(WT)*	*URA3/AmpR*
pFUS1p_STE50(6E)		*STE50(6E)*	*URA3/AmpR*
pFUS1p_STE50(6G)		*STE50(6G)*	*URA3/AmpR*
pFIG2p_STE50	*FIG2p*	*STE50(WT)*	*URA3/AmpR*
pFIG2p_STE50(6E)		*STE50(6E)*	*URA3/AmpR*
pFIG2p_STE50(6G)		*STE50(6G)*	*URA3/AmpR*
pFUS1p_STE5	*FUS1p*	*STE5(WT)*	*URA3/AmpR*
pFIG2p_STE5	*FIG2p*	*STE5(WT)*	*URA3/AmpR*
pFIG2p_STE5		*STE5(WT)*	*LEU2/AmpR*

Summary of all plasmids containing guide RNAs for gene knockout using CRISPR/Cas9		
Name	**Marker**	**gRNA Targeting site**
pCW1500	*URA3*	ATCGTTTGTTAAAGCAGTAATGG of *SST1* N-terminal coding sequence
pCW1512	*LEU2*	GTAGAATGCTCTGCTACACTTGG of *SST1* C-terminal coding sequence

pCW1683	*URA3*	GCGTCACGATCTCCACTTGGTGG of *FAR1* N-terminal coding sequence
pCW1689	*LEU2*	GAATTCTTTGCTGCTTTACCAGG of *FAR1* C-terminal coding sequence
pCW1691	*URA3*	TGCTAAGGTAGTAGACATTGCGG of *FUS1* N-terminal coding sequence
pCW1693	*URA3*	TATTCTTGGAGACAGTCACCAGG of *FUS1* C-terminal coding sequence
pCW1695	*URA3*	AATTTCCAAGTCTCTGTATAAGG of *FIG1* N-terminal coding sequence
pCW1697	*URA3*	TAGGTACAATAACTACTCTTCGG of *FIG1* C-terminal coding sequence
pCW1699	*URA3*	GCAGTGAAGTACTACTATTCTGG of *FIG2* N-terminal coding sequence
pCW1701	*URA3*	CCCATTGTCAGTACGTATGCTGG of *FIG2* C-terminal coding sequence

Table A3. Oligonucleotide Primers Used in This study

Summary of primer used for gene knockouts using CRISPR/Cas9		
Application	**Name**	**Sequence (5'-> 3')**
Bridge Template for *SST1*	OCW2062	GTGTCTAGAAGGGTCATATAATGTAAGAAATCTGGAGTACAATTTCTTTATAGC
Flanking primers for *SST1* bridge	OCW1613	CGTGATTTAATTCTAGTGGTTCGTATCGCCTAAAATCATACCAAAATAAAAAGAGTGTCTAGAAGGGTCATATAATG
	OCW1614R	TATGCTTTCCATGTATTAAAAATGACTATATATTTGATATTTATATGCTATAAAGAAATTGTACTCCAG
SST1 Verification through colony PCR	OCW2085	AGCACGTCGAGCCTTGTC
	OCW2086R	GTTCAAAATTGTGATGGCTGC
Bridge Template for *FAR1*	OCW2063	GGCGTAAGAAGGCAATCTATTAATGATAGTAGTTCGGGAATCGAGGC
Flanking primer for *FAR1* bridge	OCW2064	CTATAGATCCACTGGAAAGCTTCGTGGGCGTAAGAAGGCAATCTATTAATG
	OCW2065R	GGAGAAACGAAAAAAAAAAAAGGAAAAGCAAAAGCCTCGAAATACGGGCCTCGATTCCCGAACTACTA
FAR1 Verification through colony PCR	OCW957	ACCATCCTTTACACAAAGTC
	OCW958R	GCGTAGTATAGACGTGGAG
Summary of primers used for building *STE50* and *STE5* constructs		
Application	**Name**	**Sequence (5'-> 3')**
FIG2p amplification	OCW2018	GCGAATTGGAGCTCCACCGCGGTGGCGGCCGCTCTAGAACTAGTCAGGAGCACCAGTGC
	OCW2019R	ATCATCAACCGACCACTGGGAAAAGTCTTCATTATTCATTGCAGTTATATTCGGTAGATG
FUS1p amplification	OCW2020	GCGAATTGGAGCTCCACCGCGGTGGCGGCCGCTCTAGAACCAACAATAGTCAACAGGGC
	OCW2021R	ATCATCAACCGACCACTGGGAAAAGTCTTCATTATTCATTTTGATTTTCAGAAACTTGATGGC
FIG2p Colony PCR	OCW2018	GCGAATTGGAGCTCCACCGCGGTGGCGGCCGCTCTAGAACTAGTCAGGAGCACCAGTGC
	OCW172R	GCGAATTCTTCATTACGTCCAAGAC
FUS1p Colony PCR	OCW2020	GCGAATTGGAGCTCCACCGCGGTGGCGGCCGCTCTAGAACCAACAATAGTCAACAGGGC
	OCW172R	GCGAATTCTTCATTACGTCCAAGAC

STE5 amplification for *FIG2p* insert	OST003	CATCTACCGAATATAACTGCAATGGAAACTC CTACAGACAATATAGTTTCC
	OST001R	CGAATTCCTGCAGCCCGGGGGATCCACTAGT TCTAGAACTATGAACTTGAAAGACTAAGAAG AACTGCGTC
FIG2p amplification	OST007	GCGCAATTAACCCTCACTAAAGGGAACAAAA GCTGGAGCTCGTCAGGAGCACCAGTGC
	OST005R	GGAAACTATATTGTCTGTAGGAGTTTCCATT GCAGTTATATTCGGTAGATG
FIG2p-STE5 amplification	OST007	GCGCAATTAACCCTCACTAAAGGGAACAAAA GCTGGAGCTCGTCAGGAGCACCAGTGC
	OST001R	CGAATTCCTGCAGCCCGGGGGATCCACTAGT TCTAGAACTATGAACTTGAAAGACTAAGAAG AACTGCGTC
STE5 amplification for *FUS1p* insert	OST002	GCCATCAAGTTTCTGAAAATCAAAATGGAAA CTCCTACAGACAATATAGTTTCC
	OST001R	CGAATTCCTGCAGCCCGGGGGATCCACTAGT TCTAGAACTATGAACTTGAAAGACTAAGAAG AACTGCGTC
FUS1p amplification	OST006	GCGCAATTAACCCTCACTAAAGGGAACAAAA GCTGGAGCTCCCAACAATAGTCAACAGGGC
	OST004R	GGAAACTATATTGTCTGTAGGAGTTTCCATTT TGATTTTCAGAAACTTGATGGC
FUS1p-STE5 amplification	OST006	GCGCAATTAACCCTCACTAAAGGGAACAAAA GCTGGAGCTCCCAACAATAGTCAACAGGGC
	OST001R	CGAATTCCTGCAGCCCGGGGGATCCACTAGT TCTAGAACTATGAACTTGAAAGACTAAGAAG AACTGCGTC
Primers used for sequencing *STE50* constructs		
Application	**Name**	**Sequence (5'-> 3')**
pGAL1p_STE50(WT, 6E and 6G)	Gal1p	AATATACCTCTATACTTTAACGTC
	Cyc1t_RP	GTGAATGTAAGCGTGACAT
pFIG2p_STE50(WT, 6E and 6G)	OCW1426_T7P	TAATACGACTCACTATAGGG
	OCW172R	GCGAATTCTTCATTACGTCCAAGAC
	T3P	ATTAACCCTCACTAAAGGGA
pFUS1p_STE50(WT, 6E and 6G)	OCW1426_T7P	TAATACGACTCACTATAGGG
	OCW172R	GCGAATTCTTCATTACGTCCAAGAC
	T3P	ATTAACCCTCACTAAAGGGA

Table A4. Summary of All PCR Reactions and Their Application

PCR reaction conditions for gene knockout using CRISPR/Cas9	
PCR reaction	**PCR Reaction Conditions**
SST1 and *FAR1* Amplification of Template strand	96℃ (2’) → [94℃ (15”) → 45℃ (10”) → 72℃ (15”)] 25 cycles → 72℃ (1’30”) → 4℃ (∞)
SST1 and F*AR1* verification of gene knockout	99.9℃ (20’) → 25℃ (∞) for lysate 96℃ (2’) → [94℃ (15”) → 50℃ (10”) → 72℃ (2’15”)] 35 cycles → 72℃ (3’) → 4℃ (∞)
PCR reaction conditions for *STE50* and *STE5* constructs built	
Application	**PCR conditions**
FIG2 and *FUS1* Amplification for *STE50* constructs	96℃ (2’) → [94℃ (15”) → 50℃ (10”) → 72℃ (1’15”)] 28 cycles → 72℃ (2’) → 4℃ (∞)
pFIG2p_STE50 and *pFUS1p_STE50* Lysate	99.9℃ (20’) → 25℃ (∞)
pFIG2p_STE50 and *pFUS1p_STE50* Verification through Colony PCR	96℃ (2’) → [95℃ (15”) → 45℃ (10”) → 72℃ (1’30”)] 28 cycles → 72℃ (2’) → 4℃ (∞)
STE5 Amplification for *FIG2p* insert	98℃ (30”) → [98℃ (10”) → 62℃ (30”) → 72℃ (2’15”)] 25 cycles → 72℃ (2’) → 4℃ (∞)
FIG2p Amplification	98℃ (30”) → [98℃ (10”) → 62℃ (30”) → 72℃ (2’15”)] 25 cycles → 72℃ (2’) → 4℃ (∞)
FIG2p_STE5 Amplification	98℃ (30”) → [98℃ (10”) → 65℃ (30”) → 72℃ (3’)] 25 cycles → 72℃ (2’) → 4℃ (∞)

Table A5. Calculated Average Fluorescence Index and Standard Deviation of the Melatonin Biosensor in the Presence of 0-100 μM of Melatonin.

Plasmids Insert	[Melatonin] (μM)	Average Fluorescence Index	Standard Deviation of Fluorescence Index
Vec (*URA3*)/Vec (*LEU2*)	0	970	240
	0.01	2400	980
	0.05	22000	1400
	0.25	22000	22000
	1	670000	75000
	5	1200000	52000
	25	1700000	130000
	100	2200000	280000
***pFUS1p-STE50 (URA3)*/Vec (*LEU2*)**	0	32000	3100
	0.01	47000	2700
	0.05	140000	4200
	0.25	660000	30000
	1	1400000	100000
	5	2100000	190000
	25	2400000	140000
	100	3400000	470000
Vec (*URA3*)/*pFIG2p-STE5 (LEU2)*	0	83000	7100
	0.01	120000	6400
	0.05	210000	14000
	0.25	820000	34000
	1	1800000	15000
	5	2400000	170000
	25	3300000	130000
	100	3800000	180000
pFUS1p-STE50 (URA3) /pFIG2p-STE5 (LEU2)	0	370000	18000
	0.01	520000	21000
	0.05	960000	35000
	0.25	1900000	310000
	1	2500000	300000
	5	3900000	650000
	25	5500000	130000
	100	5400000	190000

Table A6. Calculated P-values From the Cytometry Analysis.

Plasmids Insert	**[Melatonin] (µM)**	**P-value in respect to Vec1/Vec2**	**P-value in respect to pFUS1p-STE50 /*pFIG2p-STE5***
***pFUS1p-STE50 (URA3)*/Vec (*LEU2*)**	0	0.002	0.0006
	0.01	0.0003	0.0004
	0.05	0.0003	0.0002
	0.25	0.0005	0.01
	1	0.009	0.006
	5	0.007	0.02
	25	0.0004	0.001
	100	0.05	0.006
Vec (*URA3*)/*pFIG2p-STE5 (LEU2)*	0	0.001	0.0003
	0.01	0.0007	0.0004
	0.05	0.0008	0.0005
	0.25	0.0002	0.02
	1	0.0008	0.03
	5	0.002	0.04
	25	0.0007	0.002
	100	0.0009	0.008
pFUS1p-STE50 (URA3) /pFIG2p-STE5 (LEU2)	0	0.0004	
	0.01	0.0003	
	0.05	0.0002	
	0.25	0.006	
	1	0.007	
	5	0.01	
	25	0.0008	
	100	0.003	

Table A7. Calculated Average Ratio and its Standard Deviation of the Melatonin Biosensor with Every Feedback Loop to the Control Vector at 0.05-100 µM of Melatonin.

Plasmids Insert	Concentration (µM)	Average Ratio	Standard Deviation of Ratio
pFUS1p-STE50 (URA3)/*Vec *(LEU2)	0.05	6.3	0.54
	0.25	2.9	0.24
	1	2.1	0.39
	5	1.7	0.16
	25	1.4	0.028
	100	1.6	0.44
Vec (*URA3*)/*pFIG2p-STE5 (LEU2)*	0.05	9.5	0.035
	0.25	3.7	0.27
	1	2.6	0.31
	5	1.9	0.054
	25	1.8	0.096
	100	1.8	0.17
pFUS1p-STE50 (URA3) /pFIG2p-STE5 (LEU2)	0.05	42	3.3
	0.25	8.6	2.3
	1	3.8	0.91
	5	3.2	0.63
	25	3.1	0.31
	100	2.6	0.38

Table A8. Calculated P-values From the Ratio of Each Single Feedback Loop to the Double Feedback Loop in the Melatonin Biosensor at 0.05-100 µM of Melatonin.

Plasmids Insert	Concentration (µM)	P-value in respect to *pFUS1p-STE50 /pFIG2p-STE5*
***pFUS1p-STE50* (*URA3*)/Vec (*LEU2*)**	0.05	0.001
	0.25	0.02
	1	0.02
	5	0.02
	25	0.005
	100	0.001
Vec (*URA3*)/*pFIG2p-STE5 (LEU2)*	0.05	0.002
	0.25	0.03
	1	0.04
	5	0.04
	25	0.006
	100	0.01